CATÓLICA
ESCOLA SUPERIOR DE BIOTECNOLOGIA
PORTO

EVALUATION OF ACTIVATED SLUDGE AND TREATED WATER AT WASTEWATER TREATMENT PLANT GAIA COASTLINE: PERFORMANCE INDICATORS USING PROTOZOA AND FILAMENTOUS BACTERIA

by
Luisa Fernanda Real Madrigal

July 2025

CATÓLICA
ESCOLA SUPERIOR DE BIOTECNOLOGIA
PORTO

EVALUATION OF ACTIVATED SLUDGE AND TREATED WATER AT WASTEWATER TREATMENT PLANT GAIA COASTLINE: PERFORMANCE INDICATORS USING PROTOZOA AND FILAMENTOUS BACTERIA

Dissertation presented to *Escola Superior de Biotecnologia* of the *Universidade Católica Portuguesa* to fulfil the requirements of Master of Science degree in Applied Microbiology

by
Luisa Fernanda Real Madrigal

Supervisor (Company): Engr. Ermelinda Barreiro
Tutor (University): PhD. Célia Manaia

July 2025

Dedication

I dedicate my work to my mother, who in heaven will be proud of the extent of her teachings. To my father, who always supported me unconditionally and has been an example to follow in my life. To my family, who have always been there and who have been the most beautiful constant life could have given me. To my friends, who are my family, by choice. And to my teachers, who guided me throughout my academic career. Without any of them, none of this would have been possible. And to those who are no longer here, know that their love lives on through us.

Abstract

This study analyzed the operational dynamics of the Wastewater treatment plant (WWTP) SIMDOURO S.A. in Águas de Gaia, focusing on microbial communities in the activated sludge system. Design aids odor control, but efficiency depends on the microbial population. Initially, the activated sludge process was described using the Sludge Biotic Index (SBI) to evaluate how various factors influence microfauna. The goal was to find reliable indicators for daily monitoring and assess seasonal variations in microbial communities. Sludge, Affluent, and effluent samples were collected in fall, winter, and spring, while sensors monitored dissolved oxygen (O_2) levels, temperature (Temp), and other parameters. Microscopic analysis quantified protozoan and metazoan populations, and laboratory analyses provided data on Total Suspended Solids (TSS), pH, Biochemical Oxygen Demand (COB), Chemical Oxygen Demand (COD), and nutrients like Ammonium (NH_4^+) and Nitrate (NO_3^-). Statistical analyses included t-tests, Wilcoxon tests, and Principal Component Analysis (PCA). Biological reactors 1 and 2 (T1 and T2) showed no significant differences, justifying their grouping. Seasonal shifts in microbial composition were noted: mobile ciliates dominated in autumn, while sessile ciliates prevailed in winter and spring. Key taxa such as *Epistylis* and *Microthrix* were identified, with SBI consistently at an ideal score of 10. PCA showed distinct seasonal clusters, and Modelo Linear Geral (GLM) indicated significant influences from seasonality and protozoan abundance on key parameters. Dominant filamentous bacteria included *Nocardia spp.* and *Microthrix parvicella*, correlated with specific Affluent conditions. Reliable ciliate indicators of system efficiency were identified, while flagellates and other organisms appeared sporadically. Future research should focus on advanced bacterial quantification methods, explore Artificial Intelligence (AI) and machine learning models, and extend the study into summer for a comprehensive understanding of microbial ecology.

Keywords: WWTPs; Activated sludge systems; Protozoa, Filamentous bacteria; SBI; Nutrient removal efficiency; PCA; GLM

Resumo

Este estudo analisou a dinâmica operacional de uma Estação de tratamento de águas residuais (ETAR) de SIMDOURO S.A. Vila Nova de Gaia, com foco nas comunidades microbianas no sistema de lamas ativadas. O design auxilia no controlo de odores, mas a eficiência depende da população microbiana. Inicialmente, o processo de lamas ativadas foi descrito através do Índice Biótico de Lamas (IBL) para avaliar como vários fatores influenciam a microfauna. O objetivo foi encontrar indicadores fiáveis para monitorização diária e avaliar as variações sazonais nas comunidades microbianas. Foram recolhidas amostras de lamas, afluentes e efluentes no outono, inverno e primavera, enquanto os sensores monitorizaram os níveis de oxigénio dissolvido (O_2), temperatura (Temp) e outros parâmetros. A análise microscópica quantificou as populações de protozoários e metazoários, e as análises laboratoriais forneceram dados sobre o Sólidos Suspensos Totais (TSS), pH, Demanda bioquímica de oxigénio (COB), Demanda Química de Oxigénio (COD) e nutrientes como Amônio (NH_4^+) e Nitrato (NO_3^-). As análises estatísticas incluíram testes t, testes de Wilcoxon e Análise de Componentes Principais (PCA). Reactores biológicos 1 e 2 (T1 e T2) não apresentaram diferenças significativas, justificando o seu agrupamento. Foram observadas alterações sazonais na composição microbiana: os ciliados móveis dominaram no outono, enquanto os ciliados sésseis prevaleceram no inverno e na primavera. Foram identificados táxones-chave, como *Epistylis* e *Microthrix*, com IBL consistentemente num valor ótimo de 10. A PCA mostrou grupos sazonais distintos, e os Modelos Lineares Generalizados (GLM) indicaram influências significativas da sazonalidade e da abundância de protozoários em parâmetros-chave. As bactérias filamentosas dominantes incluíram *Nocardia spp.* e *Microthrix parvicella*, correlacionadas com condições específicas de influência. Foram identificados indicadores ciliados fiáveis da eficiência do sistema, enquanto os flagelados e outros organismos apareceram esporadicamente. Pesquisas futuras devem concentrar-se em métodos avançados de quantificação bacteriana, explorar modelos de IA e aprendizagem automática e estender o estudo até ao verão para uma compreensão abrangente da ecologia microbiana.

Palavras-chave: ETARs; Sistemas de lamas ativadas; Protozoários, Bactérias filamentosas; IBL; Eficiência de remoção de nutrientes; Análise de Componentes Principais PCA; GLM

Acknowledgements

It is important to recognize SIMDOURO and its workers for providing me with a place in their facilities to carry out different practices. Dir. of Exploration João Sabino Vilaça and Tech. Manager Operations Luísa Couto Lopes who helped me in my integration process.

Recognition to the Engr. Margarida Silva and the professor Engr. Sónia Figueiredo of the ISEP - Instituto Superior de Engenharia do Porto, who helped by providing equipment and reactors during the investigation.

At last, but not least to Dr. Célia Manaia who supported me throughout the process of my mastery and in carrying out this work.

Table of contents

Abbreviations

WWTP - Wastewater Treatment Plant

SBI - Sludge Biotic Index

BRs - Biological reactors

T1 and T2 - Biological reactors 1 and 2

S2 - Sedipac 3D #2

OE – Affluent

O_2 – Dissolved oxygen, measured by Oxymax COS61D sensor

Temp – Temperature measured by Oxymax COS61D sensor

Pre – Oxygen partial pressure measured by Oxymax COS61D sensor

Sat – Oxygen saturation percentage measured by Oxymax COS61D sensor

TSS - Total Suspended Solids

COD - Chemical Oxygen Demand

COB - Biochemical Oxygen Demand

NH_4^+ - Ammonium

NH_3 - Ammonia

NO_3^- - Nitrate

Total P – Total Phosphorus

Total N - Total nitrogen

ALLSKY_SFC_SW_DWN - Downward shortwave solar radiation reaching the surface under all-sky conditions.

T2M - Air temperature measured 2 meters above ground level.

T2M_MAX - Highest daily air temperature 2 meters above ground.

T2M_MIN - Lowest daily air temperature 2 meters above ground.

PRECTOTCORR - Total precipitation corrected for systematic measurement errors.

RH2M - Relative humidity measured 2 meters above ground level.

PS - Atmospheric pressure on the Earth's surface.

PCA - Principal Component Analysis

SD - Standard Deviation

AI - Artificial Intelligence

GLM - General Linear Model

Chapter 1: Introduction

Wastewater treatment is a cornerstone of environmental protection and public health, particularly in urban areas where population growth and rising water consumption exert increasing pressure on water resources. In this context, Wastewater Treatment Plants (WWTPs) play a vital role not only in mitigating pollution but also in enabling water recovery and reuse as a strategic resource. In Portugal, for instance, average per capita water consumption exceeds the recommended value for urban areas, reaching 189 liters per day compared to the guideline of 175 L/day (Da Cunha, 2021). This scenario underscores the urgent need for efficient treatment systems and accurate monitoring strategies to ensure environmental sustainability.

Among the various biological processes employed in secondary treatment, the activated sludge system has proven to be one of the most effective ways to remove organic matter and nutrients from wastewater. This system relies on the activity of a complex microbial community, where protozoa and filamentous bacteria play key roles. Protozoa, especially ciliates, contribute to the clarification of the effluent by grazing on dispersed bacteria and serve as sensitive bioindicators of system performance. Meanwhile, filamentous bacteria are essential for floc formation and settling but can also cause operational problems such as sludge bulking or foaming when overgrown.

The Águas de Gaia WWTP, managed by SIMDOURO S.A., offers a compact and odor-controlled design that demands careful biological control to maintain optimal performance. Within this framework, the present study aimed to analyze the microbial dynamics of the activated sludge system using the Sludge Biotic Index (SBI) as a monitoring and diagnostic tool for system performance. This index allows for the assessment of treatment efficiency based on the abundance and composition of protozoan and metazoan communities.

Samples of activated sludge, Affluent, and effluent were collected across three seasons— autumn, winter, and spring— accompanied by detailed microscopic and physicochemical analyses. Additional environmental variables, such as dissolved oxygen, temperature, pressure, and saturation, were recorded via in-situ sensors. Advanced statistical methods were employed, including Principal Component Analysis (PCA) and Generalized Linear Models (GLMs), to identify seasonal patterns, determine key correlations, and isolate reliable microbial indicators of system efficiency.

By combining microbiological expertise, environmental data, and robust statistical analysis, this study contributes to a deeper understanding of microbial ecology in wastewater systems. It also provides practical insights into the application of SBI as a daily monitoring tool for operational decision-making. Moreover, the seasonal variations observed in microbial composition offer critical information for anticipating performance shifts and adjusting treatment strategies accordingly.

Ultimately, this research supports the development of smarter, more adaptive wastewater treatment systems that are both biologically informed and operationally resilient. It reinforces the importance of microbial monitoring in maintaining treatment stability, optimizing nutrient removal, and ensuring compliance with environmental regulations, thereby contributing to the broader goal of sustainable water management.

1.1. Importance of WWTP

Water is an indispensable resource for life and ecosystem stability. Despite its vital role, fresh water represents only a small fraction of the planet's total water availability—more than 96% of Earth's water is saline, with only a small portion of freshwater accessible for human use, mainly through surface and groundwater sources. In highly developed societies, the relationship between humans and water has become so embedded in everyday life that its importance is only acknowledged in moments of scarcity or when quality is compromised. For example, in mainland Portugal, the average water consumption per person is 189 L/day, surpassing the guideline value of 175 L/day for urban centers, raising serious concerns about sustainability and resource depletion. This scenario highlights the urgent need to reduce consumption and implement water reuse strategies (Da Cunha, 2021).

1.2. State of Art

One of the most impactful developments in addressing these concerns has been the implementation of WWTPs, which not only safeguard environmental health by treating effluents before discharge but also enable the recovery and potential reuse of water. Among biological treatment methods, the activated sludge process is widely used for its effectiveness in removing organic matter and nutrients from wastewater. The microbial community, particularly protozoa and filamentous bacteria, plays a critical role in the performance of these systems (Da Cunha, 2021).

In this context, microbial monitoring is essential for ensuring operational stability. The Sludge Biotic Index (SBI) has emerged as a valuable tool in assessing WWTP performance through the abundance and composition of protozoan and metazoan communities. For example, a recent study conducted in São Miguel Island concluded that "SBI has always provided important information on the abundance and density of the protozoa and metazoan community and is a valuable tool in the analysis of the performance of the WWTP" (Anjo, 2019)

Additionally, while protozoa serve as bioindicators of sludge health and process efficiency, the identification of filamentous bacteria has also been crucial in understanding sludge bulking, foaming, and other operational issues. Foam problem is often created by filamentous bacteria, such as *Nocardia spp.* (Bafghi & Yousefi, 2016).

Moreover, the application of advanced statistical models—such as General Linear Model (GLM)—has proven effective in ecological and parasitological studies, including the monitoring of European bison populations in Poland (Krzysiak et al., 2020). Inspired by these approaches, this study integrates GLM analysis to evaluate how environmental and operational factors influence the dynamics of microbial communities in a compact WWTP unit operated by SIMDOURO S.A. in Águas de Gaia.

Through microscopic and laboratory analyses across three seasons, this work aims to characterize the dominant taxa and identify reliable microbial indicators of system performance, while exploring the effects of seasonal variation on community structure. This integrated approach contributes to enhancing the understanding of microbial ecology in wastewater treatment environments.

1.3. Parts of SIMDOURO's WWTP

The Águas de Gaia WWTP, designed by the Engil – ONDEO Degrémont consortium in 2003 and dimensioned for the 2020 and 2030 horizons, treats urban wastewater through a compact, odor-controlled process that ensures regulatory compliance and operational flexibility. The scheme is organized into three integrated blocks:

Liquid line – gravity flow carries the Affluent from coarse screening through a patented Sedipac 3D unit (grit and grease removal + primary clarification) and into four-cell plug-flow aeration basins equipped with Flexazur diffusers and Dissolved Oxygen (O_2) /pH monitoring.

Effluent is degassed and settled in covered rectangular secondary clarifiers that also thicken sludge and buffer peak flows, before undergoing UV disinfection (≥ 31 mW·s cm^{-2}).

There are two Sedipac 3D facilities at the plant. Since May 16, 2024, Sedipac 3D #2 (S2) has been the only one working because Sedipac 3D #1 is undergoing maintenance. Besides being a step before entering the biological reactors (BRs), it will be soon seen other reasons for choosing this one over the affluent, specifically when working with microfauna analysis.

Sludge line – primary sludge is gravity-thickened, biological sludge is flotation-thickened; both are homogenized in a 15 m³ mixing tank (continuous agitation and degassing) and pumped to anaerobic digesters. Return activated sludge (75–150 % of Affluent flow) maintains the mass balance in the BRs. There are 2 BRs where the only difference between them is that Biological Reactor 1 (T1) alone has not been fully mixed like in Biological Reactor 2 (T2).

Air handling and odor control – local source capture and general ventilation prevent the release of NH_3, H_2S, mercaptans and aldehydes. All odor-relevant units (screens, thickeners, digesters, clarifiers) are covered, with extracted air routed to deodorization systems (Anjo, 2019) (Águas de Gaia, 2003).

1.4 Objectives

The dissertation's objectives focus on understanding activated sludge systems and SBI applications.

Key aims include examining how physicochemical, environmental, and operational variables affect microfauna communities.

Identifying effective indicators for WWTP performance and correlating SBI with environmental conditions.

Additionally, the study aimed to explore seasonal variations in microbial communities in BRs.

Chapter 2: Methodology

2.1. Sampling, Sensors, and Microbiological Analysis

2.1.1. Sampling

According to the type of analysis, samples of activated sludge and treated water, as well as from the affluent and effluent were collected at strategic points in the treatment plant, around 09:00 a.m.

During each sampling session, the samples were collected in polyethylene bottles and transported to the laboratory in a cooler. As part of the routine laboratory process from Monday to Friday, the samples were alternating on one day, taking the sample from T1 and the next from T2. On certain days, measurements were taken from the sensors of both BRs to confirm that their conditions are similar.

In total, there were 57 sampling sessions. from 11/19/2024 to 4/30/2025. To make a comparison between seasons, 8 samples were taken in Fall, 30 in Winter, and 19 in Spring.

From all these sessions the protozoan community was identified and the SBI was calculated, but the observation of filamentous bacteria began the 12/11/2024, ending the 4/29/2025. This resulted in only one sample from fall, 14 from winter, and 7 from spring. The sample size for fall would not be adequate for comparison with this season.

The S2 chemical analyses were performed every 15 days. Therefore, there is less information available. And they did not perform chemical analyses of Total Phosphorus (Total P) nor Nitrate (NO_3^-). And chemical analysis was only done on Thursdays.

The environmental data was obtained from (NASA Langley Research Center, n.d.). Where it can get the weather daily information of a certain coordinate, the same page says that the information is the average, but there is also an option to get it by hour. See **Appendix 5** to see the Root Mean Square Error (RMSE) for the parameters retrieved.

2.1.2. Sensor Characteristics

The sensors provide readings of O_2, Oxygen Partial Pressure (Pre), Saturation Percentage (Sat), and Temperature (Temp). These are then stored in the company's system for about two days. Therefore, every sampling day the BR data was also recorded at 09:00 am. The sensor used was the Endress+Hauser EH brand. According to the technical information for the Oxymax COS61D (Endress+Hauser Conducta GmbH & Co. KG, 2021), it has a maximum measured error of 0.01 mg/L or ±1% of reading for a measuring range <12 mg/L. Meanwhile, for the measuring range 12 mg/L to 20 mg/L, the maximum measured error would be ±2% of reading.

Another important features worth mentioning include its repeatability of ±0.5% of the end of the measuring range.

A) Sensor Structure and Measurement Principle (Quenching)

O_2-sensitive molecules (labels) are integrated into the optically active layer (fluorescence layer). The fluorescence layer is covered by an optical insulation layer and a cover layer. The cover layer is in direct contact with the medium.

First, the sensor optics send green light pulses to the fluorescence layer. The labels then respond (fluoresce) with red light pulses.

The duration and intensity of the response signals depend directly on the O_2 content and the hPa. All O_2 molecules are label molecules. As a result, the response signals are shorter and less intense.

The air pressure can be set via an additional sensor. The Temp of the medium is automatically recorded by the sensor. Both values are considered when calculating O_2 concentration.

2.1.3. Microscopic Analysis

Identification and relative quantification of microfauna were carried out using direct optical microscopy techniques. The microscope used was a Nikon Eclipse G200. Protozoa and metazoans were identified and quantified through direct observation alone, while bacteria were examined using Gram and Neisser staining, complemented by computational methods for filamentous bacteria identification.

A) Identification and Quantification of protozoa and metazoan

Ideally, microscopic observations should be performed within five hours of sample collection. However, when under aeration, samples may still be analyzed up to 48 hours later (Naranjo & Sandí, 2024). A homogeneous drop of the sample was examined under eyepiece magnifications of 10× and 40× for initial screening, using two replicates of 25 µL each. For small flagellates, a single 25 µL replicate was examined using a 2 µL Fuchs-Rosenthal chamber at 40× magnification. As of March 25, 2025, the Fuchs-Rosenthal chamber was replaced by the Neubauer-improved chamber.

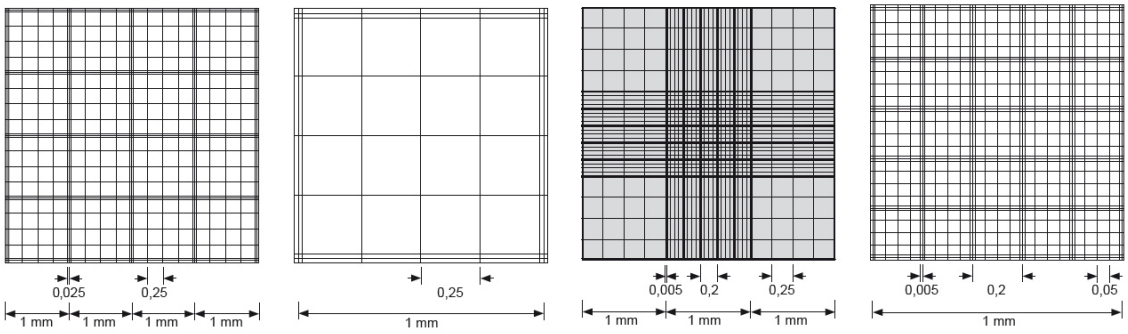

Figure 2.1 Grid Chambers for Microscopic Counting. Comparison of the Fuchs-Rosenthal chamber (0.2 mm depth) and the Neubauer-improved Blaud Brand chamber (0.1 mm depth). *Note.* Adapted from https://www.marienfeld-superior.com/rejillas-de-recuento.html

In standard procedure, the Rosenthal chamber involves counting the 1 mm² area twice diagonally, as illustrated in Figure 2.1. However, because the Neubauer chamber has a shallower depth, its 1 mm² count must be multiplied by two. In this case, rather than counting diagonally as in Figure 2.2, one of the larger quadrants located at the corners was chosen for counting.

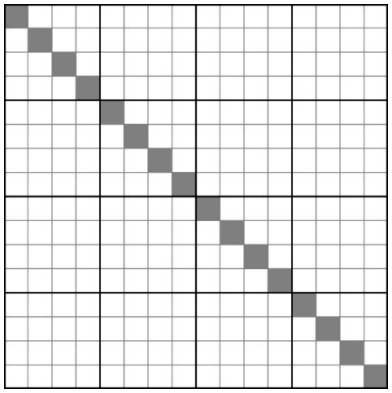

Figure 2.2 Diagram of Fuchs-Rosenthal Chamber for Flagellate Counting. Illustration of the Fuchs-Rosenthal grid chamber showing the 16 diagonally marked squares used for small flagellate quantification. *Note.* Modified from Da Cunha (2021).

Based on each sample's microscopic evaluation, the dominant group, total organism density, number of identified taxa, and flagellate count were recorded.

B) SBI

SBI for each biological sample was calculated following the methodology proposed by (Madoni, 1994). The SBI value was determined using Appendix 1, which classifies microfauna abundance and structure into corresponding quality classes. Based on the abundance estimates of protozoa and metazoa—obtained from the biological sampling process—a numerical value between 1 and 10 was assigned. This value was then translated into a classification ranging from Class I to Class IV, as detailed in Appendix 2. These classes correlate directly with the overall performance of the treatment system (Da Cunha, 2021).

C) Detection of Filamentous Bacteria

a. Gram Staining (Hucker Method)

Gram staining is a differential technique that distinguishes bacteria based on the composition and permeability of their cell walls. Gram-positive bacteria possess a thick peptidoglycan layer that effectively retains the crystal violet–iodine complex, rendering them violet or blue under the microscope. In contrast, gram-negative bacteria feature a thinner peptidoglycan layer and a more permeable outer membrane, which allows the complex to be washed out during the decolorization step. As a result, these cells absorb the counterstain safranin instead and appear pink or red. This distinction is crucial for identifying bacterial types within complex microbial communities.

One of the most sensitive aspects of the Gram staining process is the decolorization step, which must be carefully controlled and should never exceed 25 seconds. Over-decolorizing can result in even Gram-positive bacteria losing their violet coloration, leading to inaccurate classification. Additionally, aged crystal violet solutions can precipitate and produce violet, star-shaped artifacts within the field of view, which may interfere with the accuracy of observations.

In activated sludge, most filamentous bacteria stain are Gram-positive. However, exceptions are frequently observed. For instance, Type 0041 exhibits Gram-variable staining, characterized by alternating violet and red zones. This variability is often due to the presence of other bacteria attached to the trichomes, which can hinder the uniform penetration of the dye. Type 1851 tends to show weak Gram-positive staining. Other species such as *Thiothrix I, Beggiatoa*, and Type 021N are typically Gram-positive; nonetheless, when these organisms accumulate large intracellular sulfur deposits, they may present blue-stained areas that resemble a Gram-negative appearance (Strom & Jenkins, 1984).

The staining procedure began with the preparation of a thin layer of mixed liquor or foam placed onto a clean microscope slide, which was left to air dry. Once dried, the smear was completely covered with crystal violet for one minute, followed by a rinse with distilled water. Next, Gram's iodine solution was applied to the smear for one minute to act as a mordant, ensuring that the dye complex binds effectively to the cell wall. The slide was then rinsed again with distilled water. For the decolorization step, the slide was tilted at a 45-degree angle, and a 50:50 solution of acetone and ethanol (or alternatively 95% ethanol) was applied dropwise to the smear for a duration of 30 seconds. After completing the decolorization, the slide was gently blotted dry with absorbent paper. Subsequently, safranin was applied to the smear for one minute to act as the counterstain, fully covering the area. This final step was followed by a thorough rinse with distilled water and another round of blotting to remove excess moisture. The interpretation of the results was straightforward: filaments that appeared blue or violet under the microscope were identified as Gram-positive, while those that took on a pink or red coloration were identified as Gram-negative (Tripathi & Sapra, 2025).

b. Neisser Staining

Neisser staining is a method used to differentiate filamentous bacteria based on the presence of intracellular polyphosphate granules. Although the underlying biological mechanism of this technique is not entirely understood, it allows for the classification of filaments into three categories: Neisser-positive, Neisser-negative, or Neisser-positive with distinct intracellular granules. For example, *Nostocoida limicola* and Type 0092 typically exhibit a completely bluish-violet stained trichome, indicating a clear Neisser-positive reaction. Similarly, *Microthrix parvicella* and *Nocardia* also test Neisser-positive but usually present distinct intracellular granules that retain the stain. These granules, indicative of polyphosphate storage, vary in size depending on nutrient availability in the environment; in fast-growing filaments, they are generally smaller. Interestingly, bacteria such as *Hydrogenophaga hydrossis*, Type 0675, and Type 0041, which are typically Neisser-negative, can show a Neisser-positive staining pattern when cultivated under nutrient-limited conditions in activated sludge (Strom & Jenkins, 1984).

To prepare the reagents, two solutions were used. Solution 1 was composed of two parts: Solution 1A and 1B. Solution 1A consisted of Neisser's Methylene Blue Solution for microscopy (Methylene Blue Solution according to Neisser, 01263-100mL-F, Sigma-Aldrich). Solution 1B is prepared by mixing 3.3 mL of crystal violet (10% w/v in 95% ethanol), 6.7 mL of 95% ethanol,

and 90 mL of distilled water, according to (Gerardi, 2002). However, adjustments were made to match the required ethanol concentration, since 96% ethanol was used instead of 95%. In addition, Gram's 1% crystal violet solution was used instead of 10% crystal violet. The final version of Solution 1B contained 30 mL of Gram's 1% crystal violet, 4.2 mL of 95% ethanol, and 65.8 mL of distilled water. Solution 2 was prepared by mixing 33.3 mL of 1% Bismarck brown solution in distilled water with 66.7 mL of additional distilled water.

The staining procedure began by placing a drop of activated sludge on a clean microscope slide and allowing it to air dry. Once dry, the smear was covered with the freshly mixed Solution 1 for 30 seconds and then gently rinsed with distilled water. Afterwards, Solution 2 was applied and left for one minute. Following this step, the slide was rinsed thoroughly with water and gently blotted dry with absorbent paper. The interpretation of the stained samples was carried out under light microscopy. Filaments that stained bluish-violet were identified as Neisser-positive, while those appearing brown or reddish were considered Neisser-negative (Gerardi, 2002).

c. Microscopy and Image Processing

After completing the staining procedures, the prepared slides were examined using direct light microscopy under a 100× oil immersion objective. This magnification allowed for a detailed visualization of the morphological characteristics of the filamentous bacteria, which is critical for their identification.

While staining helped to preliminarily narrow down potential bacterial candidates, computational image processing was employed to achieve more precise identification by analyzing structural dimensions. This methodological approach was inspired by the work of (Dias et al., 2016), who implemented MATLAB 8.1 to detect filamentous bacteria in ISM (Imaging Scanning Microscopy) images, even when the field contained a mixture of filamentous and non-filamentous organisms. It also drew from (Oliveira & Amorim, 2024), who used ImageJ software to examine the morphological features of microbial granules.

In this study, ImageJ was selected due to the researchers' prior familiarity with the software (Rasband, 1997–present, https://imagej.net/ij/). Specifically, the Fiji distribution (fiji-windows-x64) was installed, as it provides an extensive suite of plugins tailored for scientific image analysis (Schindelin et al., 2012, https://doi.org/10.1038/nmeth.2019).

Photographs of the stained filamentous bacteria were captured using the rear camera of an OPPO Reno11 5G smartphone, which features a triple-lens system with 50MP, 32MP, and 8MP

resolutions. Because the camera was manually positioned at varying distances from the microscope eyepiece, the measurements derived from these images are considered approximate rather than exact.

To define the measurement scale, an image of the Neubauer-improved Blaud Brand counting chamber was opened in ImageJ. All subsequent images were standardized to match this scale. The image size was adjusted under the "Image > Adjust > Size" menu, with the width set to 1028 pixels. The known scale was established as 0.05 mm.

For filament length analysis, each target image was first duplicated within ImageJ to preserve the original. The duplicated image was then adjusted as needed for clarity. The Segmented Line Tool was used to trace the full outline of each filament, enabling precise length measurements. These measurements, in conjunction with the identification criteria provided in Annex 1, allowed for the tentative classification of the filaments. The outcomes were then compared to relevant literature and further contextualized using the examples shown in Annexes 7 and 8.

2.2. Physicochemical Analysis

Retrieved from laboratory manual (Simdouro, 2017) (Merck KGaA, 2021).

Table 2.1 Analytical Methods for General Parameters. The methods used to analyze general parameters were based on Simdouro protocols: ITR 4.12 R0 and ITR 4.05 R0 for the determination of total suspended solids, volatile suspended solids, and fixed suspended solids; and ITR 4.04 R0 for pH determination using the potentiometric method.

Parameter	**Total Suspended Solids (TSS)**	**pH**
Objective	This procedure defines the laboratory method for the determination of TSS.	This procedure defines the laboratory method for the analytical determination of pH in liquid and solid samples.
Principle of the Method	TSS are obtained by filtering the sample through a glass fiber filter, and then dried at 105 °C. The weight increase represents the amount of TSS.	The basic principle of potentiometric measurement is determined by the H+ activity using a standard hydrogen electrode and a reference electrode.

		pH is defined by the Sorenson scale, where its determination is calculated through −log[H+]. In practice, it is the sample acidity determination.
Interferences		Samples with high color, colloidal matter, and salinity have interference on readings with glass electrodes. temperature affects pH, so it must be recorded when reading the pH.
Reagents		Potassium Chloride (KCl) Solution = 3 M
Equipment	Analytical and precision balance Drying oven (105 °C±5 °C) Filtration ramp with vacuum	pH meter and electrode Stirring plate Analytical balance
Procedure	**Preparation of Glass Fiber Filters:** Attach the filters to the filtration device with the Buchner funnel, with the rougher surface facing up. Wash the filters with three 20 mL portions of distilled water. Remove the filters from the filtration device and transfer them to a capsule. Place the capsule with the filters in the oven at 105 °C±5 °C for 2 hours. Remove the assembly from the oven and let it cool in the desiccator. **Determination of TSS** Weigh the filter and record the value (designated P1). Attach the filter to the filtration device with the Buchner	The procedure for pH determination in liquid and solid samples is described based on the Standard Methods for the Examination of Water and Wastewater procedure. **Preparation of Pasting and Solid Sludge Samples** Weigh into a capped flask a sample amount that has approximately 5 g of dry matter, that is approximately 20 g of sludge, given the usual concentration of dehydrated sludge samples. Add distilled water so that the total weight is equal to 100 g (±1g). Place a magnetic stirrer, screw the cap tightly, and stir

	funnel, with the rougher surface facing up. Homogenize the sample, measure the necessary volume, and pour it into the filtration cup. The sample volume choice should aim for a dry residue between 2.5 mg and 200 mg. If the filtered volume does not meet the minimum requirement, increase the sample volume to be filtered up to 1 L (maximum volume). Filter the sample and place the filter in the respective previously identified watch glass. Dry in the oven at 105 °C±5 °C for 1 hour. Remove the assembly from the oven and let it cool in a desiccator. Weigh (P2) and determine TSS (*3.2*). Record the values on form Mod. 4.83. $TSS(mg/L)=V/(P2-P1)\times1000$ *(2.1)* Where: P1 – Weight of the filter (g) P2 – Weight of the filter with dry sample (g) V – Sample Volume (mL)	mechanically for at least 15 minutes, until the sample is perfectly dispersed. In some cases, it may be necessary to crush solids before mechanical agitation. Although it is preferable to use exact amounts of sludge (expressed in dry matter), this is not always possible. For speed, it may be necessary to estimate the sample's dry matter content. **Measurement** Wash the pH electrode carefully with distilled water. Dry the electrode with absorbent paper. Immediately insert the electrode into the sample. Stir the sample gently. Read and record the stabilized value by the meter on form Mod. 4.16. Remove the electrode from the sample and wash with distilled water. Once readings are complete, place the electrode in its protective sleeve with 3 M KCl.

Table 2.2 Analytical Methods for Organic Matter Oxidation. The biochemical oxygen demand (BOD_5) was determined following Simdouro protocol ITR 4.11 R0, and chemical oxygen demand (COD) was assessed using ITR 4.12 R0. Dissolved oxygen (O_2) was measured using the Oxymax COS61D sensor.

Parameter	**Biochemical Oxygen Demand (COB)**	**Chemical Oxygen Demand (COD)**

Objective	This procedure defines the laboratory process for the determination of COB.	This laboratory procedure defines the determination of COD, using Merck Spectroquant COD Cell Test Kits Ref., 1.14895.0001, and 1.14541.0001.
Principle of the Method	The COB expresses the quantity of O_2 used by the sample during a 5-day incubation period. O_2 consumed is for the biochemical degradation of organic matter, but also for the oxidation of organic compounds (e.g., nitrogen) and inorganic compounds (e.g., sulfides and Iron II), unless these processes are prevented by adding inhibitory chemicals.	The COD indicates the quantity of O_2 from potassium dichromate that reacts with the oxidizable compounds contained in 1 Liter of sample under the working conditions mentioned in the procedure. The sample is oxidized with a hot sulfuric potassium dichromate solution, using silver sulfate as a catalyst. Chlorides are masked with mercury sulfate. The concentration of unconsumed yellow chromate ion ($Cr_2O_7^{2-}$) is then determined photometrically. This test quantifies organic and inorganic compounds oxidizable by dichromate. Exceptions are some heterocyclic compounds (e.g., pyridine), quaternary nitrogen compounds, and very volatile hydrocarbons. 1 mole $K_2Cr_2O_7$ is equivalent to 1.5 mole O_2. Results are expressed in mg/L O_2.
Interferences	Oxidation of some nitrogen forms (ammonium (NH_4^+) and nitrogen oxides) constitute a strong interference	

	in the COB determination. Many factors like suspended solids presence or lack of agitation can affect the precision and accuracy of the COB determination.	
Reagents	Nitrification inhibitor N-Allylthiourea, $C_4H_8N_2S$ –5 g/L Sodium hydroxide pellets, NaOH	
Procedure	Adjust the pH in the range of 6.5 to 7.5 with diluted Hydrochloric Acid (HCl) or NaOH solutions as appropriate. According to the predicted COB value, transfer the specified sample volume to the respective bottle, as well as the nitrification inhibitor solution. Place the magnetic bar in the bottle. Place two sodium hydroxide pellets in the rubber sleeve and incorporate it into the stopper. The pellets should never be in contact with the sample. Screw the manometer to the bottle containing the sample, tightening it well to avoid leaks. Press S and M simultaneously until the display show 00. The manometer stores value every 24 hours. To read the currently recorded value, press the M button. Incubate the bottles for five days in the oven at 20 °C, with constant agitation.	Two measurement ranges were outlined, each requiring different sample volumes. **COD Range 15 – 300 mg/L** For samples in this range, 2.0 mL was pipetted into a reaction cell, sealed, and mixed vigorously. The exothermic reaction caused the cell to heat up, so handle with caution. The cell was heated at 148 °C for 2 hours, then cooled for 10 minutes before swirling and returning it to room temperature. **COD Range 25 – 1500 mg/L** For higher concentrations, 3.0 mL was used, following a similar procedure: sealing, mixing, heating at 148 °C for 2 hours, and cooling. For both procedures the cooled cells were positioned in the spectrophotometer for measurement.

	After incubation time, read the stored values. Press the S button to sequentially view the average values for each day **Appendix 3.** Convert the 5th-day value to COB using the formula: COB (mg/L)= Value indicated on display × Dilution Factor *(2.2)* Example: If a COB value between 0−200 is expected, a sample volume of 250 mL is used. The value recorded on the last of the 5 days is multiplied by factor 5.	COD concentration readings were recorded.

Note. O_2 = Dissolved oxygen, measured with the Oxymax COS61D sensor.

Table 2.3 Analytical Methods for Nutrient Determination. Nutrient concentrations were measured following Simdouro protocols: ITR 4.08 R0 for ammonia (NH_4^+), ITR 4.09 R0 for total nitrogen (N), ITR 4.14 R0 for nitrate (NO_3^-), and ITR 4.13 R0 for total phosphorus (P).

Parameter	**Ammonium (NH_4^+)**	**Total Phosphorus (Total P)**
Objective	This procedure defines the laboratory method for the determination of NH_4^+ using Merck Spectroquant NH_4^+ Cell Test Kit Ref. 1.14559.0001.	This procedure defines the laboratory method for Total P determination, using the Merck Spectroquant Phosphate Cell Test Kit Ref. 1.14729.0001.
Principle of the Method	Ammoniacal nitrogen (NH_4^+−N) is present partly as NH_4^+ and partly as ammonia (NH_3). The equilibrium between the two chemical forms depends on the pH.	In sulfuric medium, orthophosphate ions react with molybdate ions to form molybdophosphoric acid. Ascorbic acid then reduces molybdophosphoric acid to phosphomolybdenum blue

	In a strong alkaline solution, nitrogen is present almost entirely as NH_3, which reacts with hypochlorite ions and transforms into monochloramine. In turn, monochloramine reacts with a substituted phenol and forms a blue indophenol derivative that is determined photometrically. Due to the characteristic yellow color of the coloring reagent, the solution to be measured varies in color from yellowish green to green. This test determine both the concentration of NH_4^+ ions and dissolved NH_3.	(PMB), which is determined photometrically.
Interferences		This test is not suitable for determination in samples with COD concentration higher than 750 mg/L. In this case, and up to a maximum COD value of 1500 mg/L, it can be performed by adding two doses of reagent P-1K instead of one.
Procedure	The process involved checking the sample's pH to ensure it was between 4 and 13, with adjustments made using dilute sodium hydroxide or sulfuric acid if necessary. For turbid samples, filtration was performed, and dilutions were prepared as needed. After pH adjustment, 0.10 mL of the sample was pipetted into a reaction	Starting by checking the sample pH to ensure it was within the range of 0 – 10, adjusting with dilute sulfuric acid if necessary. Dilutions were prepared as needed to maintain analytical range. For digestion, 1.0 mL of the sample was pipetted into a sealed reaction cell, heated in a thermoreactor at 120 °C for

	cell, capped, and mixed. NH_4-1K reagent was added, the cell was agitated, and the mixture was allowed to react for 15 minutes. The cell was then placed in the spectrophotometer, aligned properly, and NH_4^+ concentration was recorded.	30 minutes, and allowed to cool naturally. During photometric measurement, one dose of P-1K reagent was added, mixed, followed by five drops of P-2K reagent, mixed, and left for a 5-minute reaction. Finally, one dose of P-3K reagent was added, and the cell was placed in the spectrophotometer, ensuring proper alignment. Total P concentration was recorded.

Parameter	**Nitrate (NO_3^-)**	**Total nitrogen (Total N)**
Objective	This procedure defines the laboratory method for the determination of NO_3^-, using the Merck Spectroquant NO_3^- Cell Test Kit Ref. 1.14563.0001.	This procedure defines the laboratory method for the determination of Total N, using Merck Spectroquant Total N Cell Test Kit Ref. and 1.14763.0001.
Principle of the Method	In sulfuric and phosphoric medium, NO_3^- form with 2,6-dimethylphenol the compound 4-nitro-2,6-dimethylphenol, which is determined photometrically.	Organic and inorganic nitrogen compounds are transformed into NO_3^- by the Koroleff method, reacting with an oxidant in a thermoreactor. In an acidified solution with sulfuric and phosphoric acid, NO_3^- then react with 2,6-dimethylphenol, forming 4-nitro-2,6-dimethylphenol, which is determined photometrically.
Interferences	This test is not suitable for determination in samples with chloride concentration higher than	This test is not suitable for determination in samples with chloride concentration greater than 1000 mg/L and COD greater than 700 mg/L (in the range 0.5-

	1000 mg/L and COD higher than 500 mg/L.	15 mg/L) and COD greater than 7000 mg/L (in the range 10-150 mg/L).
Procedure	The process began with pipetting 1.0 mL of the sample into a reaction cell. For turbid samples, filtration was performed beforehand. Next, 1.0 mL of NO_3^--1K reagent was added, and the cell was secured and mixed by inversion for about 15 seconds, noting that the exothermic reaction would cause the cell to heat up. After mixing, the sample was incubated for 10 minutes to ensure complete reduction of NO_3^-. The cell was then placed in the spectrophotometer, aligning the marks for accurate measurement. NO_3^- concentration was recorded.	Firstly 1.0 mL of the sample was pipetted into an empty round cell, and 9.0 mL of distilled water was added. One level blue micro spoon of N-1K reagent and six drops of N-2K reagent were added next. The cell was sealed, mixed, and heated at 120 °C for 1 hour. After heating, it cooled naturally, and the mixture was gently swirled, resulting in the "pretreated sample." For photometric measurement, 1.0 mL of the pretreated sample was added to a reaction cell, followed by 1.0 mL of N-3K reagent. After sealing the cell, it was thoroughly mixed, and the reaction was allowed to proceed for 10 minutes. The cell was then placed in the spectrophotometer, ensuring proper alignment. Total N concentration was recorded.

Note: See **Appendix 4,** for kit details including their measurement range and standard deviation.

2.3. Data Processing and Statistical Analysis (Analysis Phases)

2.3.1. PHASE 0: Pre-biological analysis

A) Comparison between BRs

The goal is to assess whether T1 and T2 can be considered equivalent, despite being measured on different days. This is necessary to justify grouping them together in the study. The comparison is based on four variables: O_2, Pre, Sat, and Temp.

Independent samples t-tests were performed for each variable to detect potential differences between T1 and T2. The analysis assumes normality and equal variances between groups.

The students' T-test was applied, provided assumptions were met. Levene's Test for equality of variances was used to verify homogeneity between groups—an essential condition for the validity of the t-test.

B) Comparison between effluent removal efficiency and S2

The dataset contains removal efficiency values for several water quality parameters (e.g., COD, NH_4^+) at two different stages of the treatment process: OE (Affluent) -effluent and S2-effluent. The main objective is to compare these two sets of values to determine whether the biological treatment and secondary clarification stages (S2-effluent) significantly contribute to the overall contaminant removal.

The Affluent–Effluent reflects the total removal efficiency of the WWTP, from raw Affluent to the final effluent. It provides a general assessment of treatment performance and regulatory compliance. Meanwhile S2–Effluent highlights the effectiveness of the biological treatment and secondary settling stages. Since S2 precedes the BRs, the comparison with the effluent helps evaluate the impact of this core part of the treatment process. This comparison is valid when using paired data collected on the same day.

Removal efficiency values for OE and S2 were organized by parameter. Difference variables were created for each parameter to assess changes between stages. The symmetry of the differences was visually explored using descriptive statistics and plots (e.g., histograms, box plots).

Due to the paired nature of the data and the lack of normality (confirmed by Shapiro-Wilk tests), the Wilcoxon Signed-Rank Test was chosen over the paired t-test. This non-parametric test is suitable for small sample sizes and non-normal distributions, which were common in the dataset.

2.3.2. PHASE 1: Data Organization and Preprocessing

First, it was needed to focus on the database structure. It centralizes all information in a single, structured database. Each row must represent a monitoring day, and each column represents a different variable. These variables include the different genera, microfauna density, small flagellates, SBI, sludge class, BRs characteristics, environmental parameters, and removal efficiency data. This was done on Microsoft Excel.

Many genus values have 0; meaning the genus was not detected in that day's sample.

2.3.3. PHASE 2: Descriptive Analysis and Contingency tables

First, Descriptive Statistics are performed for numeric variables: mean, median, SD, min, max, Interquartile Range (IQR). For Categorical Variables there were used contingency tables. Frequency followed by Crosstabs. And Test Square-Chi (χ^2) for SBI or Sludge Class vs. Season.

2.3.4. PHASE 3: Seasonal and SBI Comparisons

In this study, non-Parametric Analysis (Kruskal-Wallis) was used to compare the groups (season and SBI). This test is good for continuous variables, and this is true. If the data is not normal, Kruskal-Wallis is an excellent option. This test handles data well with a lot of data and non-normal distributions, as it is based on ranges, not on average. If it is found significant differences, follow post-hoc tests such as the Dunn test, with Holm's p-adjusted value. See **Annex 5** for the transcript used in *(Posit team, 2025)*.

2.3.5. PHASE 4: Correlations

Spearman's correlation coefficient is robust against atypical values and non-normal distributions and handles risks well. It is a good choice for the correlation matrix. Spearman option was marked (for non-normality and ceros).

2.3.6. PHASE 5: Dimension Reduction with PCA (Principal Component Analysis)

PCA was used to explore hidden patrons or clusters between samples, based on multiple variables. It allows us to summarize a lot of data in a few ways that explain most of the variability.

Data Preparation

Hellinger Transformation was performed for the microfauna (such as abundance of genera) have compositional properties dominance of a few genera, many ceros, and are not directly suitable for PCA. Hellinger's transformation softens these data by normalizing each row.

$$y'_{ij} = \sqrt{\frac{y_{ij}}{y_{i+}}} \qquad (2.3)$$

This reduces the influence of dominant genders and makes PCA more useful (Bourgeois et al., 2023)

2.3.7. PHASE 6: Predictive Modeling with GAMLj (GLM)

The study investigates the factors influencing removal efficiency in wastewater treatment, focusing on biological, environmental, and temporal aspects. It highlights the necessity of using a GLM to analyze variables such as NH_4^+ S2, P OE, and pH S2.

The primary response variable under consideration is the percentage of COD removal, with "Season" categorized as a fixed factor, including distinct levels like Spring and Summer. Continuous covariates such as the abundance of Genus X and O_2 levels are also incorporated into the analysis.

To enhance the model's predictive power, earlier findings guided the selection of predictor variables. PHASE 2 involves identifying variables that show variation in relation to removal efficiency through graphical representations. In PHASE 3, variables exhibiting significant seasonal variations are considered suitable for inclusion in the model, assessed using the Kruskal-Wallis test and Chi-squared tests.

Further, in PHASE 4, Spearman correlations are used to evaluate relationships among predictor variables. To avoid multicollinearity, only one variable from highly correlated pairs is retained, especially those with correlation coefficients exceeding 0.7 or 0.8.

Finally, PHASE 5 employs PCA to reveal patterns among samples and the microbial community by distinguishing clusters based on season or SBI. Significant principal components that account for considerable variability and are highly loaded by microbial genera are carefully examined. Additionally, the study integrates expert knowledge regarding the operation of activated sludge and WWTPs, considering historically important parameters such as dissolved O_2, Temp, pH, and organic load (Wanzer, 2023).

Chapter 3: Results

3.1. Pre-analysis results

3.1.1 Comparison between BRs

Table 3.1 Levene's Test for Homogeneity of Variance Among Biological Reactors (BRs). This table presents the results of Levene's test evaluating the equality of variances across biological reactors (BRs). The degrees of freedom for the numerator (between groups) were 1, and for the denominator (within groups), 30. The test included several parameters: O_2, temperature (Temp), oxygen partial pressure (Pre), and oxygen saturation (Sat), all measured using the Oxymax COS61D sensor. Made with Jamovi.

	F	p
O2 (mg/L)	1.77	0.19
Temp (C°)	0.15	0.70
Pre (hPa)	2.00	0.17
Sat (%)	2.08	0.16

Note. F refers to the Levene test statistic. A low *p* value suggests a violation of the assumption of homogeneity of variances. O_2 = Dissolved oxygen; Temp = Temperature; Pre = Oxygen partial pressure; Sat = Oxygen saturation percentage; all measured by the Oxymax COS61D sensor.

According to **Table 3.1** the Levene's Test p of all variables being greater than 0.05 (p>0.05), it can be assumed that there is equality of variances (homogeneity).

Table 3.2 Descriptive Statistics for Variables Measured in Biological Reactors. This table summarizes the descriptive statistics of the measured parameters (O_2, Temp, Pre, Sat) across both biological reactors (BRs 1 and 2). The total number of observations was *N* = 16. Made with Jamovi.

	BRs	O2 (mg/L)	Temp (C°)	Pre (hPa)	Sat (%)
Mean	T1	0.89	19.10	19.90	9.63
	T2	0.94	18.80	20.80	10.00
SD	T1	0.48	0.89	11.00	5.33
	T2	0.39	0.97	8.61	4.15
Median	T1	0.78	18.80	17.30	8.32
	T2	1.03	18.50	22.80	11.00
Shapiro-Wilk W	T1	0.94	0.84	0.94	0.94
	T2	0.95	0.87	0.96	0.96
Shapiro-Wilk p-value	T1	0.32	0.01	0.35	0.39
	T2	0.55	0.02	0.60	0.61

Note. SD = Standard deviation. T1 and T2 refer to Biological Reactors 1 and 2, respectively. O_2 = Dissolved oxygen; Temp = Temperature; Pre = Oxygen partial pressure; Sat = Oxygen saturation percentage; all measured by the Oxymax COS61D sensor.

In **Table 3.2,** a p-value less than or equal to 0.05 ($p \leq 0.05$) means the data are not normal. Consequently, nonparametric tests (Mann-Whitney) were used for the "Temp" variable (**Table 3.4)**. For the other variables that did follow normality, the T-student for Independent Samples was used (**Table 3.3**).

Table 3.3 Independent Samples t-Test for O_2, Pre, and Sat Between Biological Reactors. This table presents the results of the Student's *t*-tests comparing the means of O_2, Pre, and Sat between Biological Reactors T1 and T2. Degrees of freedom for all comparisons were *df* = 30. The effect size was measured using Cohen's *d*, and the standard error of the difference (SE) was reported. Made with Jamovi.

	Statistical	p	Mean Difference	EE of the difference	Effect Size
O2 (mg/L)	-0.30	0.77	-0.05	0.16	-0.10
Pre (hPa)	-0.25	0.80	-0.88	3.49	-0.09
Sat (%)	-0.24	0.82	-0.40	1.69	-0.08

Note. H_a: $\mu T1 \neq \mu T2$. Statistical = *t*-value from the Student's test. SE of the difference = Standard error. O_2 = Dissolved oxygen; Pre = Oxygen partial pressure; Sat = Oxygen saturation percentage; all measured by the Oxymax COS61D sensor.

None of the variables (O_2, Pre, nor Sat) in **Table 3.3** have significant differences ($p > 0.05$), it can be considered that T1 ≈ T2. And from here it can be seen how they behave very similarly, and it makes sense because Sat is just a percentage of O_2 concentration. And because hPa is crucial for calculating O_2 ,according to Dalton's law, it also makes sense that they behave similarly (Ahmed, 2010). So, for practical reasons, for the following statistical analyses, only O_2 was used as a proxy.

Table 3.4 Mann–Whitney U Test for Independent Variables: Temperature (°C). This table presents the results of the Mann–Whitney U test comparing temperature measurements between Biological Reactors 1 (T1) and 2 (T2), as recorded by the Oxymax COS61D sensor. The effect size is expressed using the rank-biserial correlation coefficient. Made with Jamovi.

Statistical	p	Mean Difference	EE of the difference	Effect Size
90.00	0.16	0.29		-0.30

Note. Statistical = Mann–Whitney U value. EE of the difference = standard error. H_a: μT1 ≠ μT2.

For “Temp” variable (Cohen's d of -0.297) (**Table 3.4**), although it still has a "small effect", it is closer to the "average" threshold (0.5) than the others (**Table 3.3**). However, it also can be notice that p-value for “Temp” variable is p>0.05, and it can be still argued for equivalence even though the difference is not massive, it only exists and could be something to keep into consideration.

The results of the T-student and the Mann Whitney could be argued equivalence between the groups of T1 and T2. Saying that there are no significant differences between the means of T1 and T2 for the variable in question.

3.1.2 Comparison between effluent removal efficiency and S2

In **Annex 10**, the COD Asymmetry (Skewness) is 1.161, indicating a moderately high positive skew. The Shapiro-Wilk p-value of 0.036 suggests that the data is non-normal. Consequently, it can be said that the differences for COD are non-normally distributed and exhibit moderate positive asymmetry. While the Wilcoxon test is generally robust to minor SDs, a skewness of 1.161 could still raise some concerns. It is advisable to visually inspect the histogram and boxplot of the COD differences (see **Annex 3**). The asymmetry is pronounced, and the Sign Test may serve as a more conservative alternative, albeit with less power. Nevertheless, considering that individual COD distributions for OE and S2 were borderline non-normal, the Wilcoxon test remains a viable option, though caution regarding skewness is warranted.

For COB, the Asymmetry (Skewness) is 1.91, reflecting a strong positive skew, with a Shapiro-Wilk p-value of less than 0.001, indicating high significance and strong non-normality. Therefore, the differences for COB are highly non-normal and exhibit significant positive asymmetry. In this case, the Sign Test is a much safer choice than Wilcoxon, as the latter test is sensitive to substantial SD from symmetry, making a skewness of 1.91 particularly problematic. It is important to note that the Sign Test could not be performed, as it is not available in the Jamovi software. 2.6.26 (Wanzer, 2023, https://danawanzer.github.io/stats-with-jamovi/general-linear-model.html).

In contrast, N, pH, and TSS all show low asymmetry (Skewness) and have Shapiro-Wilk p-values that are not significant, indicating that they are close to normal. Therefor the differences for these variables appear to be approximately symmetrical and near-normal, making the Wilcoxon Signed-Rank Test an excellent choice in this scenario.

Table 3.5 Paired Samples t-Test for Removal Efficiency Variables. This table summarizes the paired t-test results for removal efficiency variables between the Sedipac 3D #2 (S2) and the Affluent (OE). Variables include Total Suspended Solids (TSS), Chemical Oxygen Demand (COD), Biochemical Oxygen Demand (COB), ammonium (NH_4^+), and total nitrogen (Total N). Made with Jamovi.

mg/L	mg/L	Statistical	p
COD OE	**COD S2**	313	<.001
COB OE	**COB S2**	319	<.001
NH_4^+ OE	**NH_4^+ S2**	73	0.489
N OE	**N S2**	83.0[a]	0.060
pH OE	**pH S2**	41	0.175
TSS OE	**TSS S2**	276	0.001

Notice. H_a μMeasure 1 - Measure 2 ≠ 0, Statistical = t-test value. S2 = Sedipac 3D #2. OE = Affluent.

[a] 1 pair(s) of values are repeated

For NH_4^+, N, and pH, the biological treatment and secondary clarification (S2 to Effluent) do not show a statistically distinct removal efficiency when compared to the overall OE to Effluent removal. In **Table 3.5**, a p-value of less than 0.05 indicates a statistically significant difference between groups. This finding is particularly relevant for subsequent sections of the experiment. Due to the absence of data on NO_3^- and total P for S2, the removal efficiencies of these nutrients between OE-Efflux and S2-Efflux can be considered statistically similar. This inference is supported by the observation that the differences in removal efficiency for other nutrients, such as NH_4^+ and N, do not reach statistical significance. See **Annex 10** for Removal Efficiency Variables' means.

Additionally, it is important to remember that pH is not "removed" but rather adjusted. A "removal efficiency" metric for pH can be unusual; it often indicates the magnitude of pH change rather than removal. The means are close suggesting both stages aim to bring pH closer to a neutral range, and any difference in how much they change. It is not statistically significant **(Table 3.5)**.

Conversely, the parameters TSS and COD cannot be confidently regarded as equivalent. This distinction is logical. At this stage of the treatment process, numerous solids—including sand and grease—have been removed. This is an interesting finding, implying that the initial stages of the WWTP are highly effective for these parameters.

Looking at the means, the OE stage shows a significantly higher mean removal efficiency for TSS compared to the S2 stage. There appears to be a significant difference in COD removal efficiency. Comparing the means, the OE stage demonstrates significantly higher mean removal efficiency for COD than the S2 stage **(Table 3.5)**.

However, it seems that there is a significant difference between COB, but due to its skewness, further investigation would be necessary.

3.2. Protozoan and Metazoan Diversity: Community Composition

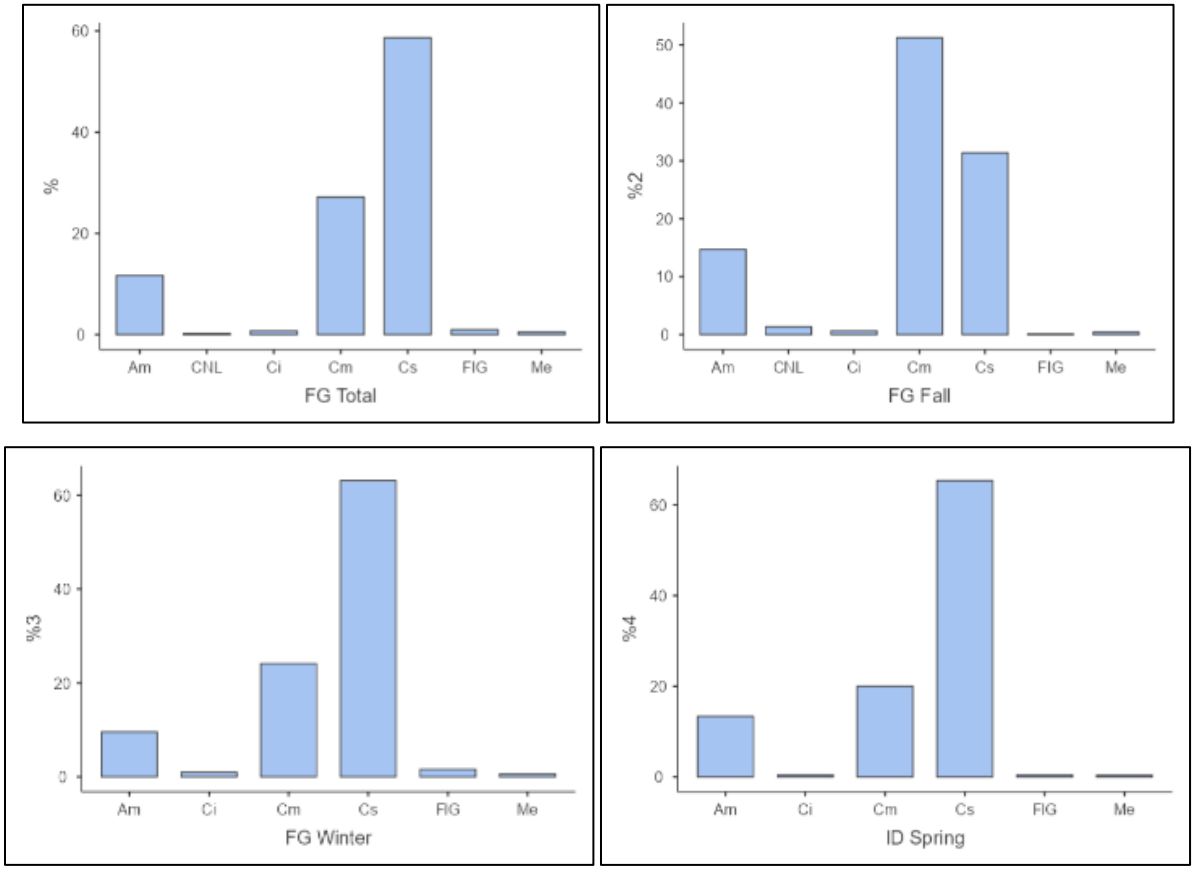

Figure 3.1. Relative Abundance of Functional Microfaunal Groups by Season. Bar graphs showing relative abundance (%) of functional groups across the entire dataset and by season (Fall, Winter, Spring).

Groups: Cs = Sessile ciliates, Cm = Bottom-mobile ciliates, Am = Thecate amoebae, FlG = Large flagellates, Ci = Carnivorous ciliates, Me = Metazoans, CNL = Free-swimming ciliates. Made with Jamovi.

When comparing community structures at the level of functional groups, a transition was noted from fall to winter and spring, with mobile ciliates (52%) being the most predominant in the fall. In winter and spring, sessile ciliates emerged as the most abundant groups, representing 63% and 65%, respectively (**Figure 3.1**).

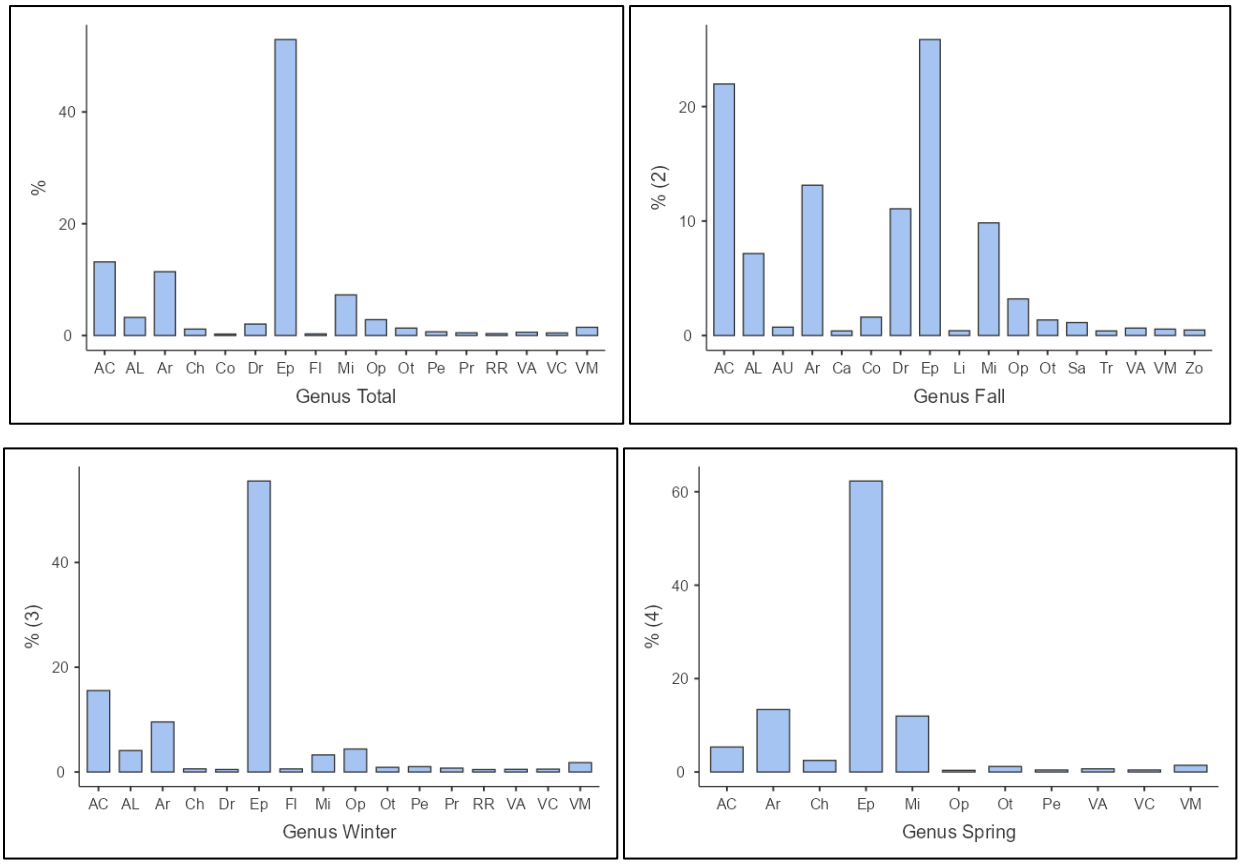

Figure 3.2. Relative Abundance of Genera by Season. Bar graphs of relative abundance (%) for microfaunal genera across all samples and seasons. Genera abbreviations include: Pe = *Peranema* spp., Fl = Unidentified flagellates, Ar = *Arcella* spp., Co = *Cochliopodium* spp., Sa = *Sathrophilus* spp., Ch = *Chilodonella uncinate*, Tr = *Trochilia minuta*, Dr = *Drepanomonas revoluta*, AC = *Aspidisca cicada*, AL = *Aspidisca lynceus*, AU = *Acineria uncinata*, Mi = *Microthorax* spp., VM = *Vorticella microstoma*, VA = *Vorticella aquadulcis*, VC = *Vorticella convallaria*, Ca = *Carchesium* spp.,

Zo = *Zoothamnium* spp., Ep = *Epistylis* spp., Op = *Opercularia* spp., Pr = *Prorodon* spp., Li = *Litonotus* spp., RR = *Rotaria* spp. (rotifers), Ot = Others. Made with Jamovi.

In **Figure 3.2** it can be appreciated that in total, the WWTP showed a strong dominance of *Epistylis spp.* (52.95%), indicating a stable and well-functioning system with good O_2 supply. The presence of *Aspidisca cicada* (13.17%) and *Arcella spp.* (11.42%) further reinforced the idea of advanced and efficient treatment, stable nitrification, and low organic loads. See **Annex 9** for examples of these protozoa.

Meanwhile in autumn, while *Epistylis spp.* was still present (25.85%), its percentage was lower, suggesting a slight shift in conditions. However, the notable increase in *Aspidisca cicada* (21.98%) and *Arcella spp.* (13.13%) pointed to even more stable nitrification and good aeration during this period.

In winter, *Epistylis spp.* surged to a very high 55.55%, strongly suggesting the plant maintained a highly stable environment despite colder temperatures. *Aspidisca cicada* (15.54%) also remained consistently present, indicating efficient treatment.

At spring, this season saw the highest percentage of *Epistylis spp.* (62.30%), signaling an exceptionally stable and well-functioning period. *Arcella spp.* (13.37%) also increased, supporting the low organic load and good aeration. Notably, the appearance and significant percentage of *Microthorax spp.* (11.97%) in spring indicated a healthy and balanced bacterial population, contributing to efficient flocculation and good effluent quality. (Canler et al., 1999)

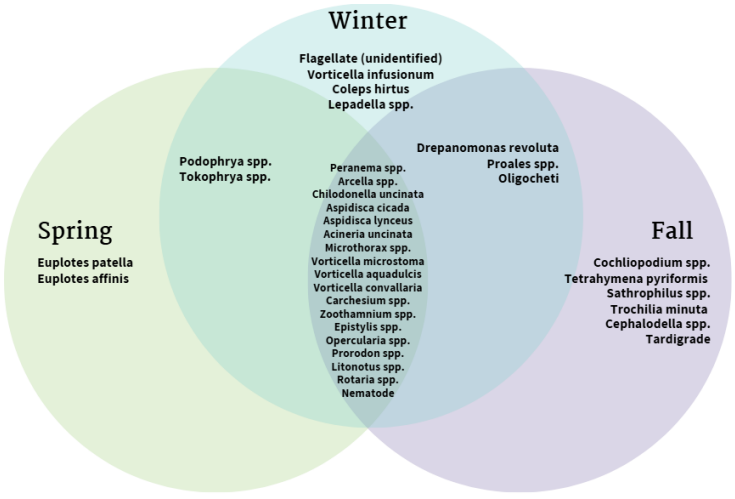

Figure 3.3. Venn Diagram of Genera Observed by Season. This figure shows the overlap and uniqueness of genera observed during each season. *Note.* Created using Canva.

From **Figure 3.3.** it is evident that certain genera persist across Spring, Winter, and Fall, suggesting they may be less susceptible to environmental changes. Additionally, there are no shared characteristic genera between Spring and Fall. This indicates a notable shift in the composition of their microfauna between these two seasons, due to a change in conditions.

3.3. Data Processing and Statistical Analysis (Analysis Phases)

3.3.1. Descriptives of all the variables and Contingency tables:

See **Annex 10**

The analysis of percentiles within the community shows notable variability and an uneven distribution of certain genera. Organisms like *Peranema spp.*, unidentified flagellates, *Tetrahymena, Cochliopodium*, and *Euplotes* were absent in 25% of samples, indicating their populations may thrive only under specific conditions, such as spikes in biodegradable organic matter or anoxic environments. This is reinforced by mean values showing these genera, along with *Vorticella, Epistylis*, and various rotifers, had a mean of zero, pointing to their absence on over half of the sampled days. Their sporadic presence seems to correlate with events like spills or seasonal changes.

Further, in the third quartile, Tetrahymena and several rotifers remained at zero in 75% of observations, suggesting they are opportunistic and depend on favorable conditions for rapid growth. In contrast, genera such as *Arcella spp.* and *Aspidisca cicada* consistently appeared, marking them as stable bioindicators of a healthy sludge ecosystem.

This diversity illustrates the ecological richness of activated sludge systems, where rare organisms may provide genetic reservoirs for resilience against environmental changes. However, the sporadic nature of some taxa complicates operational assessments, risking underestimation of their roles in nutrient removal.

Additionally, the intermittent presence of rotifers and predators hints at potential predation effects on smaller organisms, indicated by declines in COB and NH_4^+ levels during predator observations, though establishing causality would require controlled trials (Canler et al., 1999).

Table 3.6 Contingency Table of Sludge Biotic Index (SBI) by Season. This table presents the distribution of SBI values across different seasons. Made with Jamovi.

	Season			
SBI	**Fall**	**Spring**	**Winter**	**Total**
7	0	3	2	5
8	0	5	9	14
9	0	2	1	3
10	8	9	18	35
Total	8	19	30	57

Table 3.7 Chi-Square Tests for Association Between SBI and Season. This table reports the results of chi-square (χ^2) tests assessing the association between SBI and seasonal categories. Made with Jamovi.

	Valor	gl	p
χ^2	8.46	6	0.206
N	57		

Note. Degrees of freedom refer to between-group comparisons. The null hypothesis assumes no association between variables. A p-value > .05 indicates that the result is not statistically significant.

The contingency tables (**Table 3.6**) indicate that there was a prevalence of SBI 10, meaning Class I sludge. The most common sludge class identified was Class I. According to (Madoni, 1994), Class I sludge is described as very well colonized and stable, exhibiting excellent biological activity and very good performance. In contrast, Class II sludge is characterized as well colonized and stable, but with decreasing biological activity and good performance.

3.3.2 Seasonal Comparisons

See **Annex 11**

The initial statistical analysis revealed significant seasonal variations in the relative abundance of certain protozoan genera. Notably, *Chilodonella uncinata* exhibited statistically significant differences across Autumn, Spring, and Winter ($p<0.05$). Similar significant seasonal variation was also observed for *Drepanomonas revoluta*. Furthermore, an environmental covariate, downward shortwave solar radiation reaching the surface under all-sky conditions

(ALLSKY_SFC_SW_DWN), also demonstrated a statistically significant change across these seasons, suggesting its potential influence on the observed biological patterns.

3.3.3. SBI Comparisons

Instead of organizing all the variables by season, by arranging them by SBI it was obtained that the Kruskal-Wallis test indicated a significant result for *Aspidisca cicada*, with a p-value of less than 0.05. However, the subsequent Dunn test did not reveal any significant differences among the groups. It is worth mentioning that the variables NH_4^+ S2 and P OE showed significant changes shown in the Kruskal-Wallis test. Nevertheless, since data on these variables were only available for SBIs of 8 and 10, the Kruskal-Wallis test could be conducted solely for these instances.

This finding is crucial, as illustrated in the box plots (**Annex 4**), where a greater efficiency in nutrient removal corresponds with a higher SBI, which serves as a classification measure for sludge levels.

3.3.4. Correlations

The correlation map is important for the creation of the models, note that the relationship between these variables is not random. This can be seen as a p-value less than 0.05. See **Annex 6** for the table for the p-value of correlations.

3.3.5. Dimension Reduction with PCA

Together, the first two principal components (PC1 and PC2) explain 25.5% of the cumulative variance in the data. Specifically, PC1 accounts for 15.76% of the total variation, while PC2 contributes 9.7%. Although these percentages provide useful information, they indicate that these two components do not capture most of the total variability in the data (less than 50%). This suggests that a more comprehensive interpretation may necessitate considering additional dimensions—up to Dimension 6, which accounts for 51% of the cumulative variance—or that the data structure is inherently complex and cannot be easily reduced to just two principal axes.

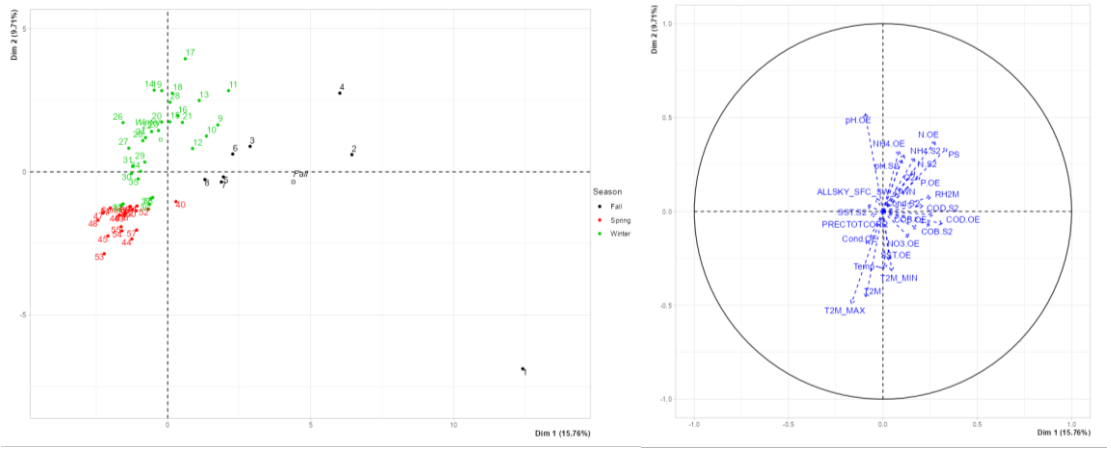

Figure 3.4. Individuals Plotted With Seasonal Categorical Variables. A visual representation of individuals colored by season as a supplementary categorical variable. Made with Jamovi.

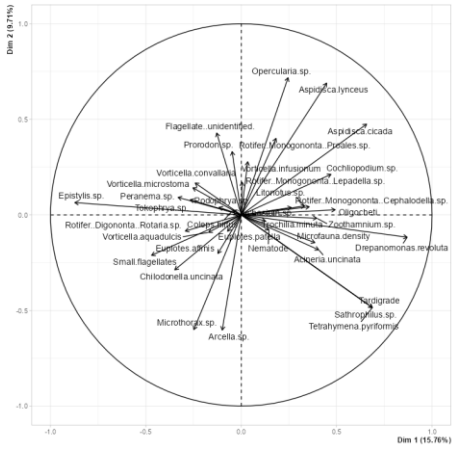

Figure 3.5 Representation of Supplementary and Active Variables. Graphical display of both active and supplementary variables from multivariate analyses. Made with Jamovi.

The PCA biplot (**Figure 3.4**) showed clear clustering of samples by season. Autumn samples were positioned toward the positive end of PC1, winter samples toward the positive end of PC2, and spring samples were associated with negative values on both dimensions.

Taxa such as Tardigrade, *Sathrophilus spp*., and *Drepanomonas revoluta* were prominent in autumn; *Opercularia* and *Aspidisca* species in winter; and *Epistylis, Microthorax*, and *Arcella* in spring. These species correspond to the longest vectors in the respective seasonal quadrants, indicating their strong contribution to seasonal clustering **(Figure 3.5)**.

Overall, the primary pattern observed was seasonal segregation of microbial communities. Other variables, such as sediment class and SBI, did not exhibit clear clustering, suggesting that they exert a weaker influence on the overall community structure.

3.3.6. Predictive Modeling with GAMLj

Table 3.8 General Linear Model Summary for Removal Efficiency Variables (mg/L). This table summarizes the GLM results for each removal efficiency variable. All values are in mg/L. Made with Jamovi.

	COD S2	COB S2	NH_4^+ S2	NO_3^- OE	P OE	N S2	pH S2	TSS S2
R-squared	1.00	1.00	1.00	0.94	1.00	1.00	1.00	0.99
Adj. R-squared	1.00	1.00	1.00	0.88	0.99	1.00	1.00	0.99

Note. S2 = Sedipac 3D #2. OE = Affluent. Variables include: TSS = Total Suspended Solids; COD = Chemical Oxygen Demand; COB = Biochemical Oxygen Demand; NH_4^+ = Ammonium; NO_3^- = Nitrate; P = Total Phosphorus; Total N = Total nitrogen.

According to **Table 3.8** and the Adjusted R-squared, this value reflects how effectively the model fits the variables. The analysis reveals that the performance for NO_3^- OE was below 0.95, which, according to (Poldrack, 2018) , probably is because only part of the data is being used to train each of the models. The results for NO_3^- OE are understandable, as the data is not sourced from S2, and incorporating S2 data could potentially enhance this value.

Table 3.9 ANOVA (Omnibus Test) for COD S2 Model. Results of the ANOVA test for the COD model at S2. Predictors include dissolved oxygen (O_2), total precipitation (PRECTOTCORR), and relative humidity (RH2M). Made with Jamovi.

	SS	df	F	p	η^2p
Model	159470.70	8.00	627.59	<.001	1.00
Season	159194.60	3.00	1670.66	<.001	1.00
Acineria uncinata	49.60	1.00	1.56	0.23	0.09

Microfauna density	177.20	1.00	5.58	0.03	0.27
O2 (mg/L)	38.00	1.00	1.20	0.29	0.07
PRECTOTCORR (mm/day)	97.50	1.00	3.07	0.10	0.17
RH2M %	46.10	1.00	1.45	0.25	0.09
Residuals	476.40	15.00			
Total	159947.10	23.00			

Note. S2 = Sedipac 3D #2. F = test statistic. SS = sum of squares. df = degrees of freedom. η^2p = partial eta squared (effect size). Residuals represent unexplained variance.

This indicates that the model at **Table 3.9** is highly significant ($p < 0.001$. Furthermore, seasonality accounts for a substantial portion of the total variability in COD S2. In this context, the density of microfauna has a considerable impact and explains a significant proportion of the variability. While the variables of *Acineria uncinata*, O_2, PRECTOTCORR, and RH2M are not statistically significant for COD, their effect sizes range from medium (>0.06) to large (>0.14). Specifically, for *Acineria uncinata*, O_2, and RH2M, the effects are medium, suggesting a possible trend that lacks statistical significance. Conversely, PRECTOTCORR exhibits a large effect size, indicating the potential for a significant relationship, even in the absence of statistical significance.

Table 3.10 Fixed Effects Parameter Estimates for COD S2 Model. This table provides model coefficients for the COD S2 model. Made with Jamovi.

			95% Confidence Interval				
Names	**Estimate**	**SE**	**Lower**	**Upper**	**β**	**t**	**p**
SeasonFall	81.87	5.57	69.99	93.74	-0.22	14.69	<.001
SeasonSpring	80.27	2.64	74.64	85.89	-0.48	30.43	<.001
SeasonWinter	85.59	2.20	80.90	90.27	0.40	38.95	<.001
Acineria uncinata	1.42	1.14	-1.00	3.85	0.34	1.25	0.23
Microfauna density	0.00	0.00	0.00	0.00	0.75	2.36	0.03
O2 (mg/L)	-3.74	3.42	-11.02	3.55	-0.29	-1.09	0.29

PRECTOTCORR (mm/day)	-1.16	0.66	-2.56	0.25	-0.49	-1.75	0.10
RH2M %	-0.40	0.33	-1.11	0.31	-0.36	-1.20	0.25

Note. df = 15. S2 = Sedipac 3D #2. O_2 = Dissolved oxygen (Oxymax COS61D sensor). PRECTOTCORR = Corrected total precipitation. RH2M = Relative humidity at 2 m.

Estimate = Unstandardized coefficient. SE = Standard error. 95% CI = Confidence interval. β = Standardized coefficient. *t* = t statistic. *p* = p-value. Scientific notation (e.g., 1.24E−06) indicates powers of ten.

All p-values for the seasons are less than 0.001, confirming the significance of seasonality **Table 3.10.** This significance is further supported by the high t-values and confidence intervals that do not include zero. The β coefficient for *Acineria uncinata* and microfauna density is positive, meaning that as these variables increase, the dependent variable COD S2 also increases. Conversely, when the variables O_2, PRECTOTCORR, and RH2M increase, COD S2 decreases. However, for RH2M, O_2, and *Acineria uncinata*, the β coefficients are smaller and not statistically significant. Despite this, the standardized β coefficient of -0.492 is substantial, suggesting that there may still be a relevant relationship, even though it is not significant.

Table 3.11 ANOVA (Omnibus Test) for COB S2 Model. Results of the ANOVA for the COB model at S2. Predictors include dissolved oxygen (O_2), maximum air temperature (T2M max), and atmospheric pressure (PS). Made with Jamovi.

	SS	df	F	p	η^2p
Model	202496.70	8.00	2732.98	<.001	1.00
Microfauna density	122.50	1.00	13.23	0.00	0.47
T2M_MAX (C°)	28.70	1.00	3.10	0.10	0.17
PS (hPa)	27.50	1.00	2.97	0.11	0.17
Season	202339.00	3.00	7282.27	<.001	1.00
Acineria uncinata	33.90	1.00	3.66	0.08	0.20
O2 (mg/L)	19.90	1.00	2.15	0.16	0.13
Residuals	138.90	15.00			
Total	202635.70	23.00			

Note. S2 = Sedipac 3D #2. F = test statistic. SS = sum of squares. df = degrees of freedom. η^2p = partial eta squared. Residuals represent unexplained variance.

This model (**Table 3.11**) demonstrates statistical significance for the dependent variable COB S2 ($p < 0.001$), with an η^2p of 0.999, indicating it nearly perfectly accounts for the variation in COB. The significant seasonal factor explains most of the variability in this dependent variable. Additionally, microfaunal density is significant, and its large η^2p effect size of 0.469 accounts for a substantial proportion of the variability. In contrast, T2M_MAX, PS, *Acineria uncinata*, and O_2 did not show statistical significance. However, T2M_MAX, PS, and *Acineria uncinata* exhibit large effect sizes, suggesting the possibility of a meaningful relationship despite the lack of statistical significance. For O_2, the effect size is medium, indicating a potential trend that does not achieve statistical significance.

Table 3.12 Fixed Effects Parameter Estimates for COB S2 Model. Model coefficient estimates for the COB S2 model. Made with Jamovi.

			95% Confidence Interval				
Names	**Estimate**	**SE**	**Lower**	**Upper**	**β**	**t**	**p**
Microfauna density	0.00	0.00	0.00	0.00	0.72	3.64	0.00
T2M_MAX (C°)	0.63	0.36	-0.13	1.39	0.50	1.76	0.10
PS (hPa)	1.67	0.97	-0.39	3.73	0.39	1.72	0.11
SeasonFall	89.65	3.26	82.69	96.60	-1.05	27.46	<.001
SeasonSpring	91.79	1.45	88.69	94.89	-0.51	63.12	<.001
SeasonWinter	95.97	1.20	93.41	98.53	0.55	79.94	<.001
Acineria uncinata	1.23	0.64	-0.14	2.60	0.45	1.91	0.08
O2 (mg/L)	-2.66	1.82	-6.54	1.21	-0.32	-1.47	0.16

Note. df = 15. S2 = Sedipac 3D #2. O_2 = Dissolved oxygen. T2M max = Maximum air temperature (2 m height). Estimate = Coefficient. SE = Standard error. 95% CI = Confidence interval. β = Standardized coefficient. *t* = t statistic. *p* = p-value.

The analysis identifies significant seasonal effects on COB S2, with Winter having the strongest positive impact (β = 0.554), while Fall (β = -1.048) and Spring (β = -0.506) show considerable decreases compared to Summer. Microfauna density emerges as a key predictor, exhibiting a significant positive correlation (β = 0.72). T2M_MAX (β = 0.503) and PS (β = 0.392) suggest tentative positive associations but are not statistically significant. *Acineria uncinata* shows a moderately large positive estimate (β = 0.45) with marginal significance (p = 0.075). In contrast, dissolved O_2 has a negative effect (β = -0.319) but is statistically inconclusive.

Table 3.13 ANOVA (Omnibus Test) for NH_4^+ S2 Model. Results of the ANOVA for the ammonium (NH_4^+) model at S2. Predictors include temperature and downward shortwave radiation under all-sky conditions (ALLSKY_SFC_SW_DWN). Made with Jamovi.

	SS	df	F	p	η^2p
Model	10782.13	12.00	1366.76	<.001	1.00
Season	6033.35	3.00	3059.19	<.001	1.00
Rotifer (Monogononta) Proales spp.	2.81	1.00	4.28	0.17	0.68
Microfauna density	725.91	1.00	1104.21	<.001	1.00
Temp (C°)	490.61	1.00	746.28	0.00	1.00
ALLSKY_SFC_SW_DWN %	126.68	1.00	192.70	0.01	0.99
Prorodon spp.	71.81	1.00	109.24	0.01	0.98
Aspidisca cicada	30.78	1.00	46.81	0.02	0.96
Acineria uncinata	9.53	1.00	14.50	0.06	0.88
Aspidisca lynceus	2.63	1.00	4.00	0.18	0.67
Chilodonella uncinata	5.99	1.00	9.11	0.09	0.82
Residuals	1.31	2.00			
Total	10783.44	14.00			

Note. S2 = Sedipac 3D #2. Temp = Temperature (Oxymax COS61D sensor). F = test statistic. SS = sum of squares. df = degrees of freedom. η^2p = partial eta squared. Residuals represent unexplained variance.

After selecting variables and exploring the data, those listed in **Table 4.22** are statistically significant for the dependent variable NH_4^+ S2. The model is highly significant ($p<0.001$) with an η^2 value of 1, indicating it explains nearly all the variation in NH_4^+ S2. Seasonality contributes

significantly to this variability ($p<0.001$, $\eta^2=1$). Other significant variables include Microfauna density ($p<0.001$, $\eta^2=0.998$), Temp ($p=0.001$, $\eta^2=0.997$), ALLSKY_SFC_SW_DWN ($p=0.005$, $\eta^2=0.99$), *Prorodon spp.* ($p=0.009$, $\eta^2=0.982$), and *Aspidisca cicada* ($p=0.021$, $\eta^2=0.959$). While Rotifer (Monogononta) *Proales spp., Acineria uncinata*, *Aspidisca lynceus*, and *Chilodonella uncinata* are not statistically significant ($p > 0.05$), their effect sizes (η^2 between 0.667 and 0.879) suggest they could have a substantial influence that deserves further investigation.

Table 3.14 Fixed Effects Parameter Estimates for NH_4^+ S2 Model. Model coefficient estimates for the NH_4^+ S2 model. Made with Jamovi.

	Estimate		95% Confidence Interval				
Names		**SE**	**Lower**	**Upper**	**β**	**t**	**p**
SeasonFall	51.39	7.91	17.38	85.41	1.58	6.50	0.02
SeasonSpring	7.44	0.91	3.54	11.34	-0.66	8.21	0.02
SeasonWinter	26.97	0.74	23.77	30.16	0.34	36.27	<.001
Rotifer (Monogononta)							
Proales spp.	8.55	4.13	-9.23	26.33	0.16	2.07	0.17
Microfauna density	0.00	0.00	0.00	0.00	0.63	33.23	<.001
Temp (C°)	-17.50	0.64	-20.26	-14.75	-0.98	-27.30	0.00
ALLSKY_SFC_SW_DW							
N %	0.02	0.00	0.01	0.02	0.25	13.88	0.01
Prorodon spp.	-3.89	0.37	-5.49	-2.29	-0.40	-10.40	0.01
Aspidisca cicada	-0.13	0.02	-0.21	-0.05	-0.18	-6.84	0.02
Acineria uncinata	2.00	0.52	-0.26	4.25	0.16	3.81	0.06
Aspidisca lynceus	0.19	0.09	-0.21	0.58	0.23	2.00	0.18
Chilodonella uncinata	-0.08	0.02	-0.18	0.03	-0.07	-3.02	0.09

Note. df = 2. S2 = Sedipac 3D #2. Temp = Temperature. ALLSKY_SFC_SW_DWN = Downward shortwave radiation. Estimate = Coefficient. SE = Standard error. 95% CI = Confidence interval. β = Standardized coefficient. *t* = t statistic. *p* = p-value.

The NH_4^+ S2 model indicates significant seasonality, with all p-values for the seasons below 0.05. Autumn has a strong positive effect (β = 1.58) on NH_4^+ S2 levels, while spring shows a relative decrease (β = -0.66). Winter also positively affects NH_4^+ S2 (β = 0.34). Microfauna density positively influences NH_4^+ S2 concentrations (β = 0.63, p < 0.001), whereas Temp has a strong negative effect (β = -0.98, p = 0.001). ALLSKY_SFC_SW_DWN positively correlates with NH_4^+ S2 (β = 0.25, p = 0.005). Some protozoa, like *Prorodon spp*. and *Aspidisca cicada*, show negative impacts on NH_4^+ S2, while *Acineria uncinata*'s effect is not significant.

Table 3.15 ANOVA (Omnibus Test) for NO_3^- OE Model. ANOVA results for the nitrate (NO_3^-) model at the Affluent (OE). Made with Jamovi.

	SS	df	F	p	η^2p
Model	3740000.00	8.00	16.57	<.001	0.94
Season	2910000.00	3.00	34.47	<.001	0.92
Small Flagellates	111805.00	1.00	3.97	0.08	0.31
Microfauna density	121700.00	1.00	4.32	0.07	0.32
Acineria uncinata	91530.00	1.00	3.25	0.11	0.27
Microthorax spp.	80317.00	1.00	2.85	0.13	0.24
Vorticella microstoma	219072.00	1.00	7.77	0.02	0.46
Residuals	253643.00	9.00			
Total	3990000.00	17.00			

Note. OE = Affluent. F = test statistic. SS = sum of squares. df = degrees of freedom. η^2p = partial eta squared. Residuals represent unexplained variance.

The NO_3OE model in Table 4.24 is highly significant (F = 16.57, p < 0.001), explaining about 94% of NO_3OE variability (η^2p = 0.936). Season is the key factor (F = 34.47, p < 0.001, η^2p = 0.92), driving most NO_3 concentration variation at the OE point. *Vorticella microstoma* is a significant predictor (F = 7.77, p = 0.021, η^2p = 0.463). Small flagellates (F = 3.97, p = 0.078, η^2p = 0.306) and microfauna density (F = 4.32, p = 0.067, η^2p = 0.324) show large effect sizes but just miss significance. *Acineria uncinata* (p = 0.105, η^2p = 0.265) and *Microthorax spp.* (p = 0.126, η^2p = 0.240) also have moderate to large effect sizes without reaching significance.

Table 3.16 Fixed Effects Parameter Estimates for NO_3^- OE Model. Parameter estimates for the NO_3^- model at OE. Made with Jamovi.

			95% Confidence Interval				
Names	**Estimate**	**SE**	**Lower**	**Upper**	**β**	**t**	**p**
SeasonFall	-362.55	176.68	-762.22	37.12	0.11	-2.05	0.07
SeasonSpring	-160.17	98.65	-383.34	62.99	0.81	-1.62	0.14
SeasonWinter	-581.41	77.57	-756.88	-405.90	-0.65	-7.50	<.001
Small Flagellates	16.71	8.39	-2.27	35.70	0.38	1.99	0.08
Microfauna density	0.00	0.00	-2.56e−6	0.00	0.42	2.08	0.07
Acineria uncinata	79.29	44.00	-20.24	178.82	0.46	1.80	0.11
Microthorax spp.	-3.66	2.17	-8.57	1.25	-0.41	-1.69	0.13
Vorticella microstoma	-24.75	8.88	-44.83	-4.67	-0.49	-2.79	0.02

Note. df = 9. OE = Affluent. Estimate = Coefficient. SE = Standard error. 95% CI = Confidence interval. β = Standardized coefficient. *t* = t statistic. *p* = p-value. Scientific notation may be used for small coefficients.

This model analyzes factors affecting NO_3^- OE. Winter is significant ($p<0.001$) with a negative β coefficient of -0.645, indicating lower NO_3^- OE compared to the baseline season. Fall ($p=0.07$) and Spring ($p=0.139$) are not significant. *Vorticella microstoma* significantly impacts NO_3^- OE ($p=0.021$) with a negative β coefficient of -0.494, suggesting that higher levels reduce NO_3^- OE. Other factors like Small Flagellates ($p=0.078$) and Microfauna density ($p=0.067$) show potential but are not statistically significant, indicating areas for further research.

Table 3.17 ANOVA (Omnibus Test) for Total Phosphorus (P) OE Model. ANOVA results for the Total Phosphorus model at the Affluent (OE). Predictors include dissolved oxygen (O_2), temperature, maximum air temperature (T2M max), total precipitation (PRECTOTCORR), and atmospheric pressure (PS). Made with Jamovi.

	SS	**df**	**F**	**p**	**η^2p**

Model	64314.60	14.00	83.22	0.01	1.00
Season	50975.70	3.00	307.82	0.00	1.00
O2 (mg/L)	2527.70	1.00	45.79	0.02	0.96
PRECTOTCORR (mm/day)	1684.60	1.00	30.52	0.03	0.94
PS (hPa)	362.10	1.00	6.56	0.13	0.77
Aspidisca cicada	212.80	1.00	3.86	0.19	0.66
T2M_MAX (C°)	3218.30	1.00	58.30	0.02	0.97
Temp (C°)	598.80	1.00	10.85	0.08	0.84
Vorticella microstoma	1786.40	1.00	32.36	0.03	0.94
Epistylis spp.	641.40	1.00	11.62	0.08	0.85
Arcella spp.	621.90	1.00	11.27	0.08	0.85
Prorodon spp.	572.10	1.00	10.36	0.08	0.84
Aspidisca lynceus	55.20	1.00	1.00	0.42	0.33
Residuals	110.40	2.00			
Total	64425.10	16.00			

Note. OE = Affluent. O_2 and Temp measured by Oxymax COS61D sensor. F = test statistic. SS = sum of squares. df = degrees of freedom. η^2p = partial eta squared. Residuals represent unexplained variance.

The refined P OE model (Table 3.17) shows strong robustness with significant Total P variability at point OE ($F = 83.22$, $p = 0.012$; $\eta^2p = 0.998$). Seasonality is the primary driver of Total P dynamics ($F = 307.82$, $p = 0.003$; $\eta^2p = 0.998$), influenced by Temp, flow, and biological activity. Dissolved O_2 ($F = 45.79$, $p = 0.021$; $\eta^2p = 0.958$) and T2M_MAX ($F = 58.30$, $p = 0.017$; $\eta^2p = 0.967$) also play critical roles. PRECTOTCORR indicates significant Total P mobilization during heavy rainfall ($F = 30.52$, $p = 0.031$; $\eta^2p = 0.938$). *Vorticella microstoma* is identified as a key bioindicator for Total P changes ($F = 32.36$, $p = 0.030$; $\eta^2p = 0.942$). Other variables show non-significant trends but have large effect sizes, while *Aspidisca cicada* suggests potential influence ($\eta^2p = 0.658$; $p = 0.189$) and *Aspidisca lynceus* has a limited effect ($\eta^2p = 0.333$; $p = 0.423$).

Table 3.18 Fixed Effects Parameter Estimates for the Total Phosphorus (P) OE Model. This table presents the coefficient estimates for the Total Phosphorus model at the Affluent (OE), with predictors

including dissolved oxygen (O_2), temperature (Temp), maximum air temperature (T2M max), total precipitation (PRECTOTCORR), and atmospheric pressure (PS). Made with Jamovi.

			95% Confidence Interval				
Names	**Estimate**	**SE**	**Lower**	**Upper**	**β**	**t**	**p**
SeasonFall	88.87	19.74	3.93	173.81	1.05	4.50	0.05
SeasonSpring	-8.57	12.75	-63.43	46.30	-2.02	-0.67	0.57
SeasonWinter	95.21	7.46	63.10	127.31	1.25	12.76	0.01
O2 (mg/L)	94.19	13.92	34.30	154.09	1.24	6.77	0.02
PRECTOTCORR (mm/day)	14.37	2.60	3.18	25.5611	1.29	5.52	0.03
PS (hPa)	22.29	8.70	-15.16	59.74	0.70	2.56	0.13
Aspidisca cicada	0.10	0.05	-0.12	0.32	0.20	1.96	0.19
T2M_MAX (C°)	16.26	2.13	7.10	25.43	1.61	7.64	0.02
Temp (C°)	-16.76	5.09	-38.67	5.14	-0.62	-3.29	0.08
Vorticella microstoma	7.40	1.30	1.80	13.00	1.38	5.69	0.03
Epistylis spp.	-0.14	0.04	-0.32	0.04	-0.75	-3.41	0.08
Arcella spp.	0.44	0.13	-0.13	1.01	0.56	3.36	0.08
Prorodon spp.	-14.61	4.54	-34.14	4.92	-0.92	-3.22	0.08
Aspidisca lynceus	0.25	0.25	-0.83	1.33	0.21	1.00	0.42

Note. df = 2. OE = Affluent. O_2 and Temp were measured using the Oxymax COS61D sensor. Estimate = Unstandardized model coefficient. SE = Standard error. 95% CI = 95% confidence interval for the coefficient. β = Standardized coefficient. *t* = t statistic. *p* = p-value. Scientific notation (e.g., 1.24E−06) indicates powers of ten.

The refined POE model (Table 3.18) is highly significant (F=83.22,p=0.012,η2p=0.998), explaining nearly all Total P variability at point OE. Seasonality is the main driver of Total P dynamics (F=307.82,p=0.003,η2p=0.998), influenced by Temp, flow, and biological activity. Other significant factors include O_2 (F=45.79,p=0.021,η2p=0.958), T2M_MAX (F=58.30,p=0.017,η2p=0.967), and PRECTOTCORR (F=30.52,p=0.031,η2p=0.938), indicating Total P mobilization during heavy rainfall. *Vorticella microstoma* (F=32.36,p=0.030,η2p=0.942) is noted as a key bioindicator. While factors like PS, Temp, *Epistylis spp.*, *Arcella spp.*, and

Prorodon spp. did not reach significance, they show notable effect sizes (η2p≥0.766). *Aspidisca cicada* may have an influence (η2p=0.658,p=0.189), while *Aspidisca lynceus* has limited impact (η2p=0.333,p=0.423).

Table 3.19 ANOVA (Omnibus Test) for the Total Nitrogen (N) S2 Model. This table displays ANOVA results for the Total Nitrogen model at Sedipac 3D #2 (S2). Predictors include O_2, temperature (Temp), downward shortwave solar radiation (ALLSKY_SFC_SW_DWN), and corrected total precipitation (PRECTOTCORR). Made with Jamovi.

	SS	df	F	p	η^2p
Model	13427.80	10.00	514.56	<.001	1.00
Season	9886.80	3.00	1262.90	<.001	1.00
Drepanomonas revoluta	63.90	1.00	24.49	0.01	0.86
Aspidisca lynceus	94.60	1.00	36.27	0.00	0.90
Small Flagellates	143.00	1.00	54.80	0.00	0.93
Microfauna density	117.10	1.00	44.88	0.00	0.92
Temp (C°)	84.60	1.00	32.43	0.01	0.89
ALLSKY_SFC_SW_DWN %	24.40	1.00	9.34	0.04	0.70
PRECTOTCORR (mm/day)	38.80	1.00	14.86	0.02	0.79
Residuals	10.40	4.00			
Total	13438.20	14.00			

Note. S2 = Sedipac 3D #2. O_2 and Temp measured by the Oxymax COS61D sensor. F = Test statistic. SS = Sum of squares. df = Degrees of freedom. η^2p = Partial eta squared (effect size). Residuals represent variance unexplained by the model.

The analysis demonstrates that the variables listed in Table 3.19 are statistically significant for the dependent variable N S2, forming a highly significant model (p<0.001) that accounts for nearly all of the variation in N S2 with an η2p value of 0.999. Seasonality is a particularly strong contributor to this variability (p<0.001,η2p=0.999). Other Affluential variables include Small Flagellates (p=0.002,η2p=0.932), Microfauna density (p=0.003,η2p=0.918), *Aspidisca lynceus*

(p=0.004,η2p=0.901), Temp (p=0.005,η2p=0.89), *Drepanomonas revoluta* (p=0.008,η2p=0.86), PRECTOTCORR (p=0.018,η2p=0.788), and ALLSKY_SFC_SW_DWN (p=0.038,η2p=0.7).

Table 3.20 Fixed Effects Parameter Estimates for the Total Nitrogen (N) S2 Model. This table presents coefficient estimates for the Total Nitrogen model at S2.

			95% Confidence Interval				
	Estimate		Lower	Upper			
Names		**SE**			**β**	**t**	**p**
SeasonFall	-38.42	18.53	-89.86	13.03	-3.86	-2.07	0.11
SeasonSpring	27.58	1.77	22.66	32.51	0.07	15.55	<.001
SeasonWinter	34.68	1.52	30.44	38.91	0.49	22.74	<.001
Drepanomonas revoluta	5.00	1.01	2.19	7.80	1.26	4.95	0.01
Aspidisca lynceus	0.32	0.05	0.17	0.46	0.45	6.02	0.00
Small Flagellates	-0.89	0.12	-1.23	-0.56	-0.35	-7.40	0.00
Microfauna density	0.00	0.00	0.00	0.00	0.31	6.70	0.00
Temp (C°)	-7.80	1.37	-11.60	-4.00	-0.51	-5.69	0.01
ALLSKY_SFC_SW_DWN %	-0.01	0.00	-0.02	0.00	-0.13	-3.06	0.04
PRECTOTCORR (mm/day)	0.79	0.20	0.22	1.35	0.14	3.85	0.02

Note. df = 4. S2 = Sedipac 3D #2. Temp = Temperature. ALLSKY_SFC_SW_DWN = Downward shortwave solar radiation. PRECTOTCORR = Corrected total precipitation. Estimate = Unstandardized coefficient. SE = Standard error. 95% CI = Confidence interval. β = Standardized coefficient. *t* = t statistic. *p* = p-value.

The analysis of predictors influencing N S2 highlights the significant role of seasonality. Both spring and winter show highly significant effects ($p < 0.001$), with high t-values (15.55 for spring and 22.74 for winter) and positive estimates (27.58 for spring and 34.68 for winter), indicating a substantial increase in N S2 during these seasons. In contrast, fall is not statistically significant

($p = 0.107$), but its negative β coefficient (–3.86) suggests a potential decrease in N S2 that may warrant further investigation.

In addition to seasonality, several environmental and biological factors significantly influence N S2 levels. *Drepanomonas revoluta* ($p = 0.008$, $\beta = 1.26$) and *Aspidisca lynceus* ($p = 0.004$, $\beta = 0.45$) are positively associated with N S2. Small Flagellates ($p = 0.002$, $\beta = –0.35$) show a significant negative relationship. Other relevant variables include Microfauna density ($p = 0.003$, $\beta = 0.31$), Temp ($p = 0.005$, $\beta = –0.51$), ALLSKY_SFC_SW_DWN ($p = 0.038$, $\beta = –0.13$), and PRECTOTCORR ($p = 0.018$, $\beta = 0.14$), all of which contribute meaningfully to explaining N S2 variability.

Table 3.21 ANOVA (Omnibus Test) for the pH S2 Model. ANOVA results for the pH model at S2. Predictors include O_2, air temperature (T2M), corrected total precipitation (PRECTOTCORR), and relative humidity (RH2M). Made with Jamovi.

	SS	df	F	p	η^2p
Model	132.83	14.00	2497.10	0.02	1.00
Season	71.52	3.00	6274.00	0.01	1.00
T2M (C°)	8.71	1.00	2292.50	0.01	1.00
Small Flagellates	10.19	1.00	2682.50	0.01	1.00
PRECTOTCORR (mm/day)	12.28	1.00	3230.60	0.01	1.00
Microfauna density	18.59	1.00	4891.90	0.01	1.00
O2 (mg/L)	5.70	1.00	1499.10	0.02	1.00
RH2M %	7.38	1.00	1943.10	0.01	1.00
Arcella spp.	0.25	1.00	65.20	0.08	0.99
Aspidisca cicada	1.10	1.00	288.90	0.04	1.00
Microthorax spp.	0.47	1.00	125.00	0.06	0.99
Prorodon spp.	0.31	1.00	81.70	0.07	0.99
Opercularia spp.	0.19	1.00	51.20	0.09	0.98
Residuals	0.00	1.00			
Total	132.84	15.00			

Note. S2 = Sedipac 3D #2. O_2 measured by Oxymax COS61D sensor. F = Test statistic. SS = Sum of squares. df = Degrees of freedom. η^2p = Partial eta squared. Residuals represent unexplained variation.

The analysis shows that the variables listed in Table 3.21 significantly influence pH S2. The overall model is highly significant ($p = 0.016$) and explains nearly all variance ($\eta^2p = 1$). Seasonality is a major factor ($p = 0.009$, $\eta^2p = 1$), along with Microfauna density, PRECTOTCORR, Small Flagellates, and T2M are statistically significant ($p \leq 0.013$) and accounting for nearly all variability ($\eta^2p = 1$). RH2M and O_2 also have very strong effects ($p = 0.014$ and 0.016, $\eta^2p = 0.999$), while *Aspidisca cicada* is significant ($p = 0.037$, $\eta^2p = 0.997$).

Although *Microthorax spp.*, *Prorodon spp.*, *Arcella spp.*, and *Opercularia spp.* are not statistically significant ($p > 0.05$), their high effect sizes ($\eta^2p = 0.981–0.992$) indicate they could still be relevant and should be examined further with a larger sample size.

Table 3.22 Fixed Effects Parameter Estimates for the pH S2 Model. This table presents the fixed effects coefficients for the pH model at S2. Made with Jamovi.

			95% Confidence Interval				
Names	**Estimate**	**SE**	**Lower**	**Upper**	**β**	**t**	**p**
SeasonFall	6.00	0.11	4.59	7.42	1.79	53.88	0.01
SeasonSpring	-1.01	0.13	-2.60	0.58	-1.44	-8.09	0.08
SeasonWinter	3.96	0.09	2.87	5.06	0.85	45.91	0.01
T2M (C°)	-0.68	0.01	-0.86	-0.50	-0.79	-47.88	0.01
Small Flagellates	0.38	0.01	0.29	0.47	1.12	51.79	0.01
PRECTOTCORR (mm/day)	-0.98	0.02	-1.21	-0.76	-1.32	-56.84	0.01
Microfauna density	0.00	0.00	0.00	0.00	2.72	69.94	0.01
O2 (mg/L)	-4.64	0.12	-6.16	-3.12	-0.94	-38.72	0.02
RH2M %	-0.37	0.01	-0.47	-0.26	-0.86	-44.08	0.01
Arcella spp.	-0.03	0.00	-0.07	0.02	-0.34	-8.07	0.08
Aspidisca cicada	-0.02	0.00	-0.03	0.00	-0.24	-17.00	0.04
Microthorax spp.	-0.03	0.00	-0.06	0.00	-0.43	-11.18	0.06
Prorodon spp.	0.14	0.02	-0.06	0.35	0.13	9.04	0.07
Opercularia spp.	0.03	0.00	-0.02	0.07	0.21	7.16	0.09

Note. df = 1. S2 = Sedipac 3D #2. T2M = Air temperature. RH2M = Relative humidity. O_2 = Dissolved oxygen. Estimate = Coefficient. SE = Standard error. 95% CI = Confidence interval. β = Standardized coefficient. *t* = t statistic. *p* = p-value.

The analysis of pH S2 reveals that both seasonal and environmental factors significantly influence its levels. Fall (p = 0.012) and Winter (p = 0.014) are associated with higher pH S2 values compared to the reference season, while Spring shows a non-significant negative trend (p = 0.078).

Among environmental variables, T2M, PRECTOTCORR, RH2M, and O_2 show significant negative effects on pH S2, suggesting that higher this variables levels reduce pH. In contrast, Small Flagellates and Microfauna density have significant positive effects, with Microfauna showing a particularly strong influence (β = 2.722) despite a small raw estimate.

Although some biological variables like *Arcella spp.*, *Microthorax spp.*, *Prorodon spp.,* and *Opercularia spp.* do not reach statistical significance (p > 0.05), their consistent trends and large effect sizes suggest they may play a role and should be further explored with a larger dataset.

Table 3.23 ANOVA (Omnibus Test) for Total Suspended Solids (TSS) S2 Model. ANOVA results for the TSS model at S2. Predictors include O_2, T2M, PRECTOTCORR, and RH2M. Made with Jamovi.

	SS	df	F	p	η^2p
Model	132.83	14.00	2497.10	0.02	1.00
Season	71.52	3.00	6274.00	0.01	1.00
T2M (C°)	8.71	1.00	2292.50	0.01	1.00
Small Flagellates	10.19	1.00	2682.50	0.01	1.00
PRECTOTCORR (mm/day)	12.28	1.00	3230.60	0.01	1.00
Microfauna density	18.59	1.00	4891.90	0.01	1.00
O2 (mg/L)	5.70	1.00	1499.10	0.02	1.00
RH2M %	7.38	1.00	1943.10	0.01	1.00
Arcella spp.	0.25	1.00	65.20	0.08	0.99
Aspidisca cicada	1.10	1.00	288.90	0.04	1.00
Microthorax spp.	0.47	1.00	125.00	0.06	0.99
Prorodon spp.	0.31	1.00	81.70	0.07	0.99

Opercularia spp.	0.19	1.00	51.20	0.09	0.98
Residuals	0.00	1.00			
Total	132.84	15.00			

Note. S2 = Sedipac 3D #2. O_2 = Dissolved oxygen measured using the Oxymax COS61D sensor. TSS = Total Suspended Solids. F = Test statistic. SS = Sum of squares. df = Degrees of freedom. η^2p = Partial eta squared. Residuals represent unexplained variance.

The analysis indicates that the variables in Table 3.23 significantly influence TSS S2. The model is statistically significant ($p = 0.016$) and explains nearly all variation in the dependent variable ($\eta^2p = 1$). Seasonality is a major contributing factor ($p = 0.009$, $\eta^2p = 1$), along with Microfauna density, PRECTOTCORR, Small Flagellates, T2M, RH2M, and O_2, all showing strong significance ($p \leq 0.016$) and very high effect sizes ($\eta^2p \geq 0.999$). *Aspidisca cicada* is also significant ($p = 0.037$, $\eta^2p = 0.997$). Although *Microthorax spp., Prorodon spp., Arcella spp.*, and *Opercularia spp.* are not statistically significant ($p > 0.05$), their high effect sizes ($\eta^2p = 0.981–0.992$) suggest they may still be relevant and merit further investigation with a larger sample size.

Table 3.24 Fixed Effects Parameter Estimates for Total Suspended Solids (TSS) S2 Model. This table presents the fixed effect coefficient estimates for the TSS model at S2. Made with Jamovi.

			95% Confidence Interval				
Names	**Estimate**	**SE**	**Lower**	**Upper**	**β**	**t**	**p**
SeasonFall	80.90	5.91	68.37	93.42	-0.47	13.69	<.001
SeasonSpring	80.26	3.52	72.80	87.72	-0.54	22.80	<.001
SeasonWinter	89.01	2.94	82.77	95.25	0.48	30.26	<.001
Microfauna density	0.00	0.00	0.00	0.00	0.83	2.71	0.016
O2 (mg/L)	-12.34	4.60	-22.09	-2.59	-0.68	-2.68	0.016
PRECTOTCORR (mm/day)	-2.32	0.89	-4.21	-0.44	-0.70	-2.62	0.019
RH2M %	-0.97	0.45	-1.92	-0.02	-0.61	-2.16	0.046

Note. df = 16. S2 = Sedipac 3D #2. O_2 = Dissolved oxygen. PRECTOTCORR = Corrected total precipitation. RH2M = Relative humidity. Estimate = Coefficient. SE = Standard error. 95% CI = Confidence interval. β = Standardized coefficient. *t* = t statistic. *p* = p-value.

The analysis reveals that several variables significantly influence TSS S2. The model is highly significant, with a partial eta-squared (η^2p) of 1, meaning it explains nearly all variability in TSS S2. Seasonality also has a major impact, alongside variables like Microfauna density, PRECTOTCORR, Small Flagellates, T2M, and RH2M, all showing strong effects ($p = 0.014$, $\eta^2p = 1$). O_2 also has a very large effect ($p = 0.016$, $\eta^2p = 0.999$), and *Aspidisca cicada* is significant ($p = 0.037$, $\eta^2p = 0.997$). While *Microthorax spp.*, *Prorodon spp., Arcella spp.,* and *Opercularia spp.* are not statistically significant ($p > 0.05$), their high effect sizes ($\eta^2p = 0.981–0.992$) suggest they may still be relevant, warranting further investigation with a larger sample size.

Several ciliates identified as statistically significant predictors in the linear models—such as *Aspidisca cicada, Vorticella microstoma, Drepanomonas revoluta, Aspidisca lynceus, Microthorax spp.*, and *Prorodon spp.*—are in alignment with previous literature that associates their presence with specific operational and environmental conditions in the WWTP. *Aspidisca cicada*, frequently highlighted in this analysis, is commonly interpreted as an indicator of well-functioning, nitrifying systems with low NH_3 levels, supporting its role in predicting high treatment efficiency. Similarly, *Vorticella microstoma*, often found in systems with moderate organic load, reflects environments rich in free-living bacteria, potentially linking its presence to fluctuations in suspended solids and organic matter. The detection of *Prorodon spp.*, typically associated with low NH_4^+ concentrations and stable nitrification, also supports its relevance as an indicator of advanced treatment performance. Overall, the significance of these taxa in the models reinforces their ecological roles described in the literature and highlights their potential use as bioindicators of operational efficiency in activated sludge systems (Canler et al., 1999).

3.4. Relative abundance of bacteria

Regarding bacterial quantification, it is important to note that the findings were not the result of a standardized or rigorously validated methodology. Instead, they emerged from a qualitative, exploratory process based on visual observation and tentative identification based on microscopic observations. Bacteria were identified and categorized according to a numerical scale (Annex 2), indicating their relative abundance. The most frequently observed filamentous bacteria were *Nocardia* spp. and similar organisms (38 counts), *Microthrix parvicella* (27 counts), and Type 0041 (26 counts). These findings align with known bioindicator characteristics.

Nocardia spp. are associated with high sludge age, well-aerated conditions, warmer temperatures, and complex Affluents like oils and fats. *Microthrix parvicella* thrives in low mass loading, low O_2, and lipid-rich Affluents, preferring slightly alkaline conditions (optimal around pH 8). Type 0041 indicates floc dispersion and is linked to high sludge age and low mass loading in urban wastewater, with potential nutrient deficiencies in industrial systems (Isac, Rodríguez, Salas, & Fernández, 2008). See Annex 7 for examples of these bacteria observed.

During the staining process, it was observed that some of the reagents for Neisser Staining were available were expired. In addition to that the crystal violet dye used also contained phenol (C_6H_5OH) at 4 g/L. Although they were still used with caution, this limitation may have affected the staining quality and, consequently, the clarity of bacterial morphology under the microscope. Such constraints underscore the importance of reagent integrity in microbiological analyses.

Given the early stage of this bacterial analysis and the limited number of samples available, drawing comparisons across different sampling stations may not yet be appropriate.

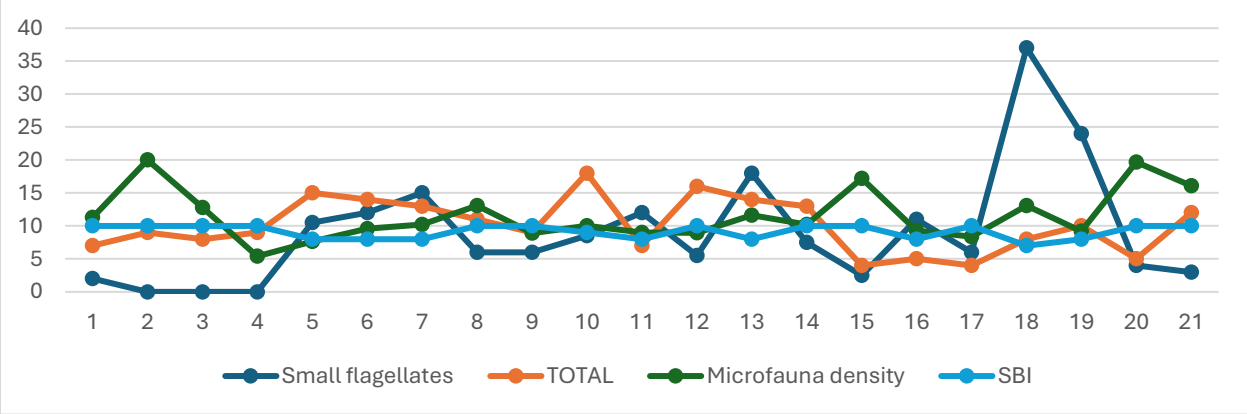

Figure 3.6. Temporal Dynamics of Microbial Biota and SBI. This figure illustrates the changes in the biotic community and corresponding SBI scores over time.

To facilitate trend analysis, large-magnitude variables, such as microbial density, were transformed. The initial analysis focused on the relationship between bacterial observations and variables related to the activated sludge community **(Figure 3.6).** Interestingly, small flagellates appeared to exhibit a synchronous increase with the relative observation of bacteria. Conversely, both microfauna density and SBI tended to decrease as the relative bacterial count increased. This inverse relationship aligns with existing literature, which suggests that certain protozoa primarily graze on

filamentous bacteria, potentially leading to an increase in their populations as bacterial abundance lowers (Canler et al., 1999).

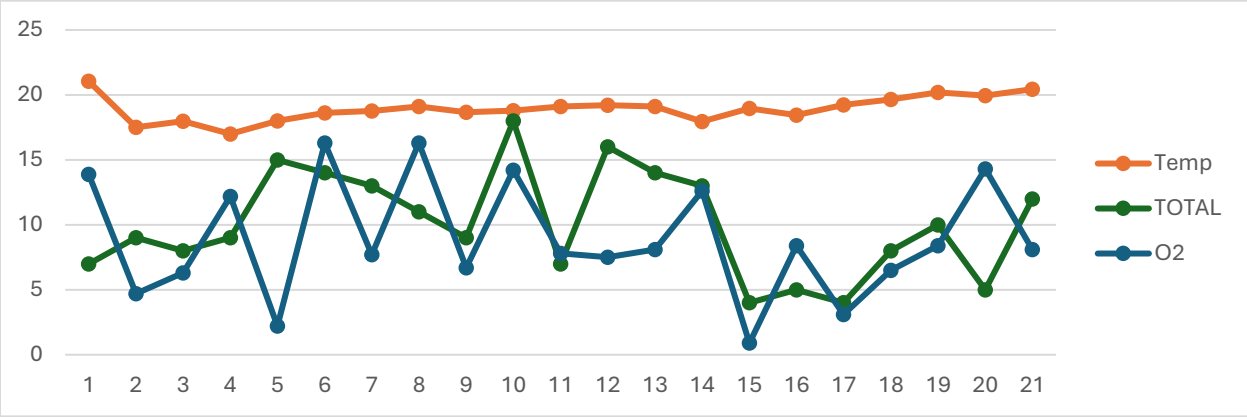

Figure 3.7. Filamentous Bacteria Dynamics and Biological Reactor Variables. Temporal trends of filamentous bacteria and biological reactor (BR) factors (e.g., O_2, Temp).

The relationship between bacterial presence and the physicochemical characteristics of the RBs presented a more complex picture. Regarding Temp, inverse influence or the involvement of other confounding factors, warranting further investigation. In contrast, a reciprocal relationship was observed with dissolved O_2 (**Figure 3.7**).

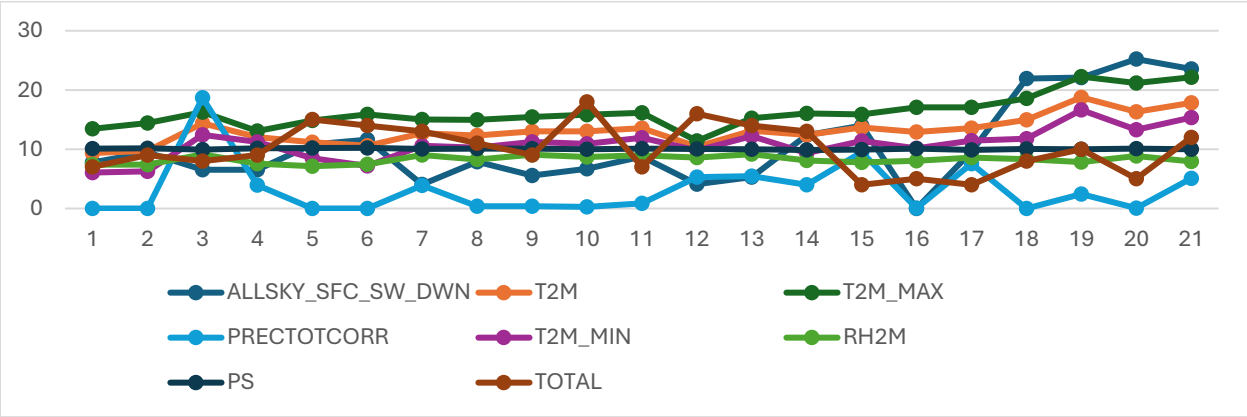

Figure 3.8 Filamentous Bacteria and Environmental Variables Over Time. Trends of filamentous bacteria presence in relation to environmental parameters.

Environmental factors also showed discernible patterns in relation to bacterial presence. Factors that increased in conjunction with bacterial observations included ALLSKY_SFC_SW_DWN,

suggesting a potential link between solar radiation and bacterial growth or activity. Conversely, the following factors tended to decrease as bacterial observations increased: T2M, T2M_MAX, PRECTOTCORR, T2M_MIN, RH2M, and PS. These inverse relationships could indicate environmental conditions that become less favorable for certain bacterial populations, or perhaps a competitive dynamic where increased bacterial activity alters these local environmental parameters (**Figure 3.8**).

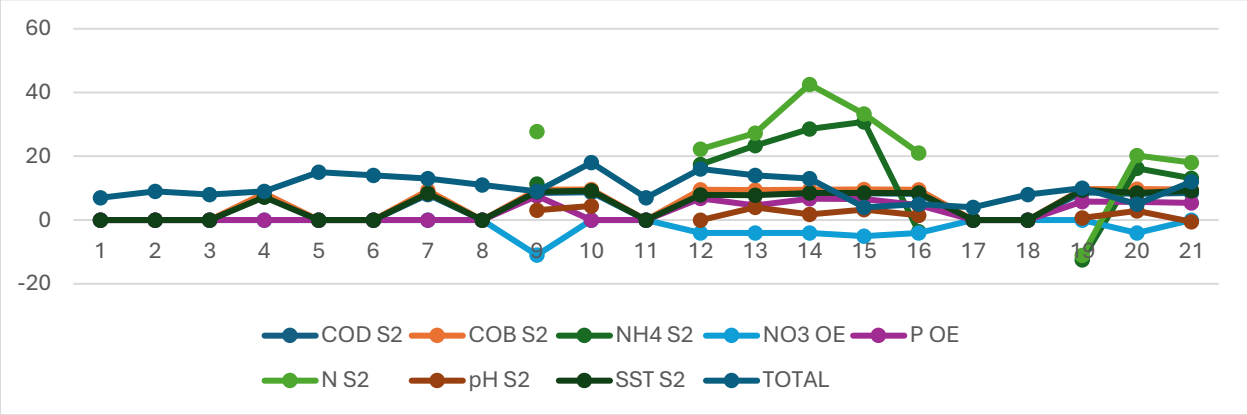

Figure 3.9 Filamentous Bacteria and Removal Efficiency Variables Over Time. This figure shows the relationship between filamentous bacteria dynamics and wastewater removal efficiency metrics.

Finally, regarding removal efficiency, a positive correlation was observed between NO_3^- OE and increasing bacterial presence. This suggests that the bacteria present play a significant role in NO_3^- removal processes. Conversely, NH_4^+ S2, N S2, pH S2 , and P OE appeared to increase when bacterial observations decreased. This might indicate that different bacterial communities or processes are responsible for these removal efficiencies, or that high bacterial loads (as qualitatively observed) might sometimes hinder these specific removal pathways. The relatively small changes observed in COD S2, COB S2, and TSS S2 suggest that these parameters were less influenced by the qualitative variations in bacterial presence at this stage of the process, which is a positive indication of consistent effluent quality (**Figure 3.9**).

These findings align with Assunção (2013), who noted that abundant filamentous bacteria were linked to poor sludge settleability. These high levels of filamentous bacteria, together with protozoan identification and measurements, indicated potential reductions in effluent quality and highlighted operational issues.

The current study supports that excessive filamentous bacteria growth may affect removal processes and indicate system instability. Although COD and TSS were stable, changes in nitrogen-related parameters suggest microbial imbalances.

Chapter 4: Conclusions

This study investigated the year-round performance of a WWTP by integrating physico-chemical monitoring with an analysis of the activated sludge micro-fauna.

Physico-chemically, the study found that parameters like temperature, pH, and key nutrients (NH_4^+, total N, total P, and NO_3^-) showed minimal changes between the initial (OE) and final (S2) control points, suggesting that the second polishing step had limited additional impact on these variables. Notably, significant reductions in TSS and COD were observed early in the treatment process at OE, indicating that the bulk of pollution removal occurred in the initial stages.

From a biological perspective, distinct seasonal patterns emerged. Mobile ciliates were prominent in autumn, while sessile forms such as *Epistylis* and *Arcella* thrived during colder months and spring, signaling stable and well-aerated conditions. The appearance of Microthorax in spring indicated a balanced bacterial food supply and good effluent quality. The SBI consistently remained at 10, underscoring the stability and health of the biomass throughout the year.

Multivariate analyses provide deeper insights. Although the first two PCA axes explained only 25% of the total variance, they effectively differentiated seasonal dynamics, highlighting the multi-factorial nature of the system. GLM analyses confirmed that season, temperature, and protozoan density were crucial drivers of pollutant removal, particularly for COD at S2 and Total N forms. Several ciliates, including *Aspidisca cicada, Vorticella microstoma, Drepanomonas revoluta, Microthorax spp.,* and *Prorodon spp.*, were identified as significant predictors, consistent with their known roles as bioindicators of stable, nitrifying conditions.

The study also offered critical operational insights from the distribution of filamentous bacteria. *Nocardia spp., Microthrix parvicella*, and Type 0041 were the most frequently observed, correlating with specific system conditions like high sludge age, aeration levels, temperature, and nutrient imbalances, suggesting that their overgrowth is linked to environmental and operational stressors. A potential competitive relationship between filamentous bacteria and protozoa was observed, with increased filament abundance often coinciding with a decline in SBI and protozoan density, supporting the idea that protozoa graze on filaments. Environmental variables like

ALLSKY_SFC_SW_DWN were linked to filament proliferation, while higher O_2 seemed to suppress them. Better NO_3^- removal was associated with more filaments, whereas more efficient removal of NH_4^+, Total N, Total P, and neutral pH occurred when filaments were less dominant.

Finally, the analysis of community percentiles revealed uneven distribution of various genera, with some taxa like *Tetrahymena, Cochliopodium, Peranema spp.*, and unidentified flagellates, along with rotifers and predators, appearing sporadically, suggesting responses to specific disturbances or opportunistic ecological effects.

In conclusion, the wastewater treatment system performed effectively year-round, with performance strongly influenced by seasonal changes and microbial community dynamics. Since OE handles most pollutant removal, operational optimization efforts (e.g., aeration and sludge age) could primarily target this initial zone, while S2 could serve as a fine-tuning stage. The consistent monitoring of specific protozoan groups could offer a cost-effective early-warning system for process stability. This study emphasizes the value of integrated monitoring approaches for understanding the complex interactions within full-scale activated sludge systems, despite certain data limitations.

Chapter 5: Future work

Future research on wastewater treatment systems should focus on improving bacterial measurement techniques, such as using Quantitative Polymerase Chain Reaction (qPCR) and photography programs like ImageJ for cost-effective quantification, especially filamentous bacteria. The integration of Artificial Intelligence (AI) and machine learning can aid in identifying effective statistical models and analyzing key variables for better predictive accuracy.

Increasing the sample size for S2 and using alternative analysis methods could enhance insights into removal efficiencies. Exploring seasonal variations, particularly during summer, would provide a comprehensive view of system performance.

While qualitative assessments of bacteria offer valuable comparisons, detailed quantitative studies are needed to clarify relationships between bacterial communities, physicochemical properties, and treatment efficiency. As the methodology is further developed, ensuring the use of validated and up-to-date reagents will be critical for improving accuracy and reproducibility.

Additionally, further investigation into other environmental factors and specific protozoa, even those not statistically significant, could reveal important insights.

Bibliography

Águas de Gaia, E.M. (2003). *Memória descritiva e dimensionamento processual para o horizonte de projecto 2020: ETAR de Gaia Litoral* (Version 2.0, verified by HT, September 19, 2003). Engil, ONDEO Degrémont.

Ahmed, T. (2010). Chapter 2: Equilibrium ratios. In T. Ahmed (Ed.), *Working guide to vapor-liquid phase equilibria calculations* (pp. 5–7). Gulf Professional Publishing. https://doi.org/10.1016/B978-1-85617-826-6.00002-9

Anjo, M. D. C. M. A. (2019, October 25). *Caracterização das comunidades de protozoários e metazoários em ETAR domésticas e industriais de São Miguel: relação de eficiência de remoção e condições de operação* [Master's thesis, Universidade dos Açores]. RepositóriUM. http://hdl.handle.net/10400.3/5417

Assunção, P. C. C. (2013). *Controlo analítico da ETAR de Serzedo e avaliação do desempenho da instalação* [Master's thesis]. Universidade do Minho, Escola de Engenharia. https://repositorium.sdum.uminho.pt/bitstream/1822/35369/1/Paula%20Cristina%20Cunha%20Assun%C3%A7%C3%A3o.pdf

Bafghi, M. F., & Yousefi, N. (2016). Role of *Nocardia* in activated sludge. *Malaysian Journal of Medical Sciences, 23*(3), 86–88. https://www.ncbi.nlm.nih.gov/pmc/articles/PMC4934723/

Bourgeois, B., Giroux-Bougard, X., Winegardner, A., Chrétien, E., Granados, M., & Braga, P. H. P. (2023, April 24). *Chapter 10: Transformations*. In QCBS R Workshop Series, Quebec Centre for Biodiversity Science. Retrieved July 7, 2025, from https://r.qcbs.ca/workshop09/book-en/transformations.html

Canler, J. P., Perret, J.-M., Duchene, P., & Cotteux, E. E. (1999). Aide au diagnostic des stations d'épuration par l'observation microscopique des boues activées. https://doi.org/10.34894/VQ1DJA

Da Cunha, A. S. (2021). *Integração do índice biótico de lamas na avaliação da qualidade do tratamento de águas residuais por lamas ativadas: Caso de estudo*. [Master's thesis, University of Minho, School of Engineering].

Dias, P. A., Dunkel, T., Fajado, D. A. S., Gallegos, E. D. L., Denecke, M., Wiedemann, P., Schneider, F. K., & Suhr, H. (2016). Image processing for identification and

quantification of filamentous bacteria in in situ acquired images. *BioMedical Engineering Online, 15*(1), Article 64. https://doi.org/10.1186/s12938-016-0197-7

Endress+Hauser Conducta GmbH & Co. KG. (2021, November 10). *Operating instructions: Oxymax COS61D dissolved oxygen sensor*. [Technical manual]. Retrieved from https://bdih-download.endress.com/files/DLA/005056A500261EDC978414DCF261CC23/BA00460CEN_1721-00.pdf

Gerardi, M. H. (2002). *Settleability problems and loss of solids in the activated sludge process* [e-book]. **John Wiley & Sons, Inc.** https://doi.org/10.1002/047147164X

Isac, L., Rodríguez, E., Salas, M. D., & Fernández, N. (2008). *Ficha: Bacterias filamentosas en el fango activo* (Grupo Bioindicación Sevilla [GBS], Practical Manual, Chapters 157–192). Grupo Bioindicación Sevilla. https://www.bibliotecagbs.com/archivos/157_192_CAPficha_BACTERIAS.pdf

Krzysiak, M. K., Demiaszkiwicz, A. W., Larska, M., Tomana, J., & Anusz, K. (2020). Parasitological monitoring of European bison (*Bison bonasus*) from three forests of north-eastern Poland between 2014 and 2016. *Journal of Veterinary Research (Poland)*, *64*(1), 103–110. https://doi.org/10.2478/JVETRES-2020-0022

Madoni, P. (1994). A sludge biotic index (SBI) for the evaluation of the biological performance of activated sludge plants based on the microfauna analysis. *Water Research, 28*(1), 67–75. https://doi.org/10.1016/0043-1354(94)90120-1

Merck KGaA. (2021, April). *Operating manual: Spectroquant® Prove spectrophotometer* (Version 3.0 – 04/2021). [Technical manual]. Retrieved from https://www.sigmaaldrich.com/deepweb/assets/sigmaaldrich/product/documents/383/650/sq-prove-operating-manual-en-2021-04.pdf

Naranjo, M. L., & Sandí, W. B. (2024). Índice biológico de lodos como bioindicador en dos sistemas de tratamiento de agua residual hospitalaria en Costa Rica. *UNED Research Journal*, *16*, e5334. https://doi.org/10.22458/urj.v16i1.5334

NASA Langley Research Center. (n.d.). *Prediction of Worldwide Energy Resources (POWER): Data Access Viewer & data services*. Retrieved July 6, 2025, from https://power.larc.nasa.gov/data-access-viewer/

Nicolau, A. (2008, January). *Identificação de problemas ao nível do decantador e controlo do crescimento filamentoso – 1º nível* [Training presentation]. FILOUT2008, Instituto Superior Técnico.

Oliveira, A. T., & Amorim, C. L. (2024). *BAS – Lab Class 3: Microscopic observation and evaluation of activated sludge from wastewater treatment plants* [Laboratory guide]. Universidade Católica Portuguesa, Porto.

Paul Marienfeld. (n.d.). *Rejillas de recuento*. Retrieved July 6, 2025, from https://www.marienfeld-superior.com/rejillas-de-recuento.html

Poldrack, R. A. (2018). The general linear model (Chap. 14). In *Statistical Thinking for the 21st Century* (M. Mejía, T. Nuño, & L. Reyes, Trans.). Retrieved from https://statsthinking21.github.io/statsthinking21-core-spanish-site/the-general-lineal-model.html

Posit team. (2025). *RStudio: Integrated Development Environment for R* [Software]. Posit Software, PBC. Retrieved from https://posit.co/downloads/

Rasband, W. (1997–present). *ImageJ* [Software]. National Institutes of Health & LOCI, University of Wisconsin–Madison. Retrieved from https://imagej.net/ij/

Schindelin, J., Arganda-Carreras, I., Frise, E., Kaynig, V., Longair, M., Pietzsch, T., ... & Cardona, A. (2012). Fiji: an open-source platform for biological-image analysis. *Nature Methods, 9*(7), 676–682. https://doi.org/10.1038/nmeth.2019

Simdouro, S.A. (2017). *Instrução de trabalho ITR 4.04–4.14* [Internal technical procedures]. Vila Nova de Gaia, Portugal: Simdouro, S.A.

Statorials. (2023). *Post hoc tests for the Kruskal-Wallis-test in R*. Retrieved from https://www.youtube.com/watch?v=pyLQmUfrel8

Strom, P. F., & Jenkins, D. (1984). Identification and significance of filamentous microorganisms in activated sludge. *Journal of the Water Pollution Control Federation, 56*(5), 449–459. http://www.jstor.org/stable/25042271

Tripathi, N., & Sapra, A. (2025). Gram Staining. In *StatPearls*. StatPearls Publishing. http://europepmc.org/books/NBK562156

Wanzer, D. (2023). *General linear model*. *Statistics with jamovi*. https://danawanzer.github.io/stats-with-jamovi/general-linear-model.html

Appendices and annexes

Appendices

Appendix 1 Two-Way Table for Sludge Biotic Index (SBI) Classification. This appendix shows the criteria used to determine SBI scores based on microfaunal key groups, density, and the number of taxonomic units. Retrieved from Da Cunha, A. S. (2021)

Dominant Group	**Density (ind/L)**	**S>10**		**8≤S≤10**		**5≤S≤7**		**S<5**	
		F<10	**10<F<100**	**F<10**	**10<F<100**	**F<10**	**10<F<100**	**F<10**	**10<F<100**
Ciliates (bottom mobile) + Sessile and/or Amoebas with Teak	≥10^6	10	8	9	7	8	6	7	5
	<10 ^6	9	7	8	6	7	5	6	4
Ciliates (sessile) (>80%)	≥10 ^6	9	7	8	6	7	5	6	4
	<10 ^6	8	6	7	5	6	4	5	3
Opercullaria spp.	≥10 ^6	7	5	6	4	5	3	4	2
	<10 ^6	6	4	5	3	4	2	3	1
Vorticella Microstoma	≥10 ^6	6	4	5	3	4	2	3	1

	<10 ^6	5	3	4	2	3	1	2	0
Ciliates (free swimmers)	≥10 ^6	5	3	4	2	3	1	2	0
	<10 ^6	4	2	6	1	2	0	1	0
Small Flagellates (>100)	≥10 ^6	4		3		2		1	
	<10 ^6	3		2		1		0	

Appendix 2 SBI Quality Classification Table. This appendix presents the conversion of SBI values into four qualitative classes indicating treatment performance. Retrieved from Da Cunha, A. S. (2021)

Value SBI	Class
8-10	I
6-7	II
4-5	III
0-3	IV

Appendix 3 Volume Correspondence Table for Biochemical Oxygen Demand (COB). This appendix includes detailed correspondence of volume measurements for COB testing and analysis. Retrieved from Simdouro, S.A. (2017).

Sample Volume (mL)	COB Range (mg/L)	Dilution Factor	Nitrification Inhibitor Solution (number of drops)
432	0−40	1	9
365	0−80	2	7
250	0−200	5	5
164	0−400	10	3
97	0−800	20	2

43.5	0−2000	50	1
22.7	0−4000	100	1

Appendix 4 Kit Details for Ammonium (NH_4^+) Analysis. Information retrieved from Millipore Sigma (n.d.), detailing analytical kits used for NH_4^+ quantification. Concentration values are based on diluted and ready-to-use standard solutions.

Ref.	**Total range (**mg/L)	**Concentration (**mg/L)	**Expanded measurement Uncertainty (**mg/L)
1.14895.0001	15 – 300 COD	100	± 3
		200	± 4
1.14541.0001	25 – 1500 COD	100	± 3
		200	± 4
		400	± 5
		1000	± 11
1.14559.0001	4.0 – 80.0 NH_4^+-N	6.00	± 0.13
		12.0	± 0.4
		50.0	± 1.2
1.14729.0001	0.5 – 25.0 P	4.00	± 0.08
		15.0	± 0.4
1.14563.0001	0.5 – 25.0 NO_3^--N	2.50	± 0.06
		15.0	± 0.4
		10.0	± 0.3
		50.0	± 2.0
1.14763.0001	10 – 150 N	12.0	± 0.3
		100	± 3

Appendix 5 Summary of Root Mean Square Error (RMSE) for Atmospheric and Radiative Parameters. This appendix presents RMSE values used in model validation for parameters including solar radiation (ALLSKY_SFC_SW_DWN), temperature (T2M, T2M max, T2M min), relative humidity

(RH2M), and surface atmospheric pressure (PS). Retrieved July 6, 2025, from https://power.larc.nasa.gov/data-access-viewer/

Parameter	Source	Value	Units
ALLSKY_SFC_SW_DWN	GEWEX SRB	13.5 (All Sites), 36.5 (60° Poleward), 12.1 (60° Equatorward)	%
T2M	MERRA-2	2.11	°C
T2M_MAX	MERRA-2	3.1	°C
T2M_MIN	MERRA-2	3.15	°C
PRECTOTCORR	MERRA-2	3.69	mm/day
RH2M	SL-AV Model	0.1 (observation error standard deviation)	% (implied)
PS (hPa)	MERRA-2	1.82	hPa

Note. RMSE indicates the average magnitude of model prediction errors relative to observed values.

Annexes

Annex 1 Summary of Filamentous Bacteria Observed During the Experiment. This annex provides a modified version of Strom and Jenkins (1984, Table 1), limited to the filamentous bacteria observed in this study and the most common taxa in municipal wastewater treatment systems. Additional source: Nicolau (2008).

Species	Diameter (µm)	Compression (µm)	Filament Shape	Cell Shape	Filament Location	Bath	Sesseus Growth
***Nostocoida limicola* I**	0.6–0.8	100–200	Enrolled / irregular	Spherical / discoid	External / internal / free	No	No
***Nostocoida limicola* II**	1.2–1.4	100–200	Enrolled / irregular	Cane oval / spherical / discoid	External / internal / free	No	No
***Nostocoida limicola* III**	1.6–2.0	200–300	Enrolled / irregular	Cane oval / spherical / discoid	External / internal	No	No

T 1851	0.8	100–300	Straight / curved	Rectangular	External	Yes	Yes
T 0961	0.8–1.4	>500	Right	Rectangular	External	No	No
T 0092	0.8–1.0	10–60	Straight / bent	Rectangular	Internal	No	No
T 0803	0.8	50–150	Straight / curved	Rectangular	External / free	No	No
T 0411	0.8	50–150	Doubled / lev. curved/irregular	Oval cane	External	No	No
T 1701	0.6–1.0	20–200	bent / curved lev.	cane with rounded end	external / internal	Yes, not very visual	yes
T 0041	1.2–1.9	100–500	straight / curved / bent	square / rectangular	external / internal	yes	yes
T 021N	0.8–2.2	100–>1000	direito / lev. curved/rolled	discoid /square/ rectangular/barrel	external	no	no
***Thiotrix* I**	1.4–2.5	100–500	straight / curved	rectangular	external	yes	no / yes
***Thiotrix* II**	0.7–1.4	50–200	straight / curved	rectangular	external	yes	no / yes
T 0914	0.7–1.0	50–200	straight / curved	square	external / free	no	no
Beggiatoa spp.	1.0–3.0	100–500	straight / curved	rectangular/cell not visible	external / free	no	no
Mycothrix parvicella	0.6–1.0	100–400	enrolled / irregular	invisible cell	internal / free	no	no
Type 0581	0.4–0.7	100–200	enrolled	invisible cell	internal / free	no	no
***Nocardia spp.* and similar**	1	10–20	branch	invisible cell	internal / free	no	no

T 1863	0.8	20–50	irregular	oval stick	external / internal / free	no	no

Species	**Inclusions of ensofre**	**Other Inclusions**	**Gram stain**	**Neisser Coloring, Filam**	**Neisser Coloring, Granule**	**Density of the Septum**	**Branchings**	**Mobility**
***Nostocoida limicola* I**	No	No	+	+	-	No	No	No
***Nostocoida limicola* II**	No	Yes	-,+, +/-	+, -	-	Yes	No	No
***Nostocoida limicola* III**	No	Yes	-,+, +/-	+, -	-	Yes	No	No
T 1851	No	No	+ weak	-	-	No	No	No
T 0961	No	No	-	-	-	No	No	No
T 0092	No	Yes	-	+	-	No	No	No
T 0803	No	No	-	-	-	No	No	No
T 0411	No	No	-	-	-	Yes	No	No
T 1701	no	Yes	-	-	-	no (yes, at the end two filaments)	no	No
T 0041	no	Yes	+, +/- -, +/- (associated with enxofre)	+,-	+, -	no	no	No
T 021N	yes (spherical)	Yes	)	-	+, -	yes	no	vibrant
***Thiotrix* I**	yes (spherical)	Yes	-,+	-	+, -	no	no	vibrant
***Thiotrix* II**	yes (spherical)	Yes	-,+	-	+, -	no	no	vibrant

	yes							
T 0914	(spherical)	Yes	-,+	-	+, -	no	no	No
Beggiatoa	yes							
spp.	(spherical)	Yes	+, -	-	+, -	no	no	yes
Mycothrix								
parvicella	no	Yes	+	-	+, -	no	no	No
T 0581	no	no	-	-	-	no	no	No
Nocardia								
***spp*.** **and**								
similar	no	Yes	+	-	+, -	no	yes (true)	No
T 1863	no	Yes	-	-	+, -	yes	no	No

Annex 2 Presence and Relative Abundance of Filamentous Bacteria (Genera and Types) by Sampling Date. This annex lists filamentous bacteria identified during the study period, categorized by: 1. Observed presence, 2. Common occurrence, and 3. Predominance in samples.

Date	T 0961	T 0411	T 1701	T 1863	T 1851	T 0041	*Nostocoida limicola* I	*Nostocoida limicola* II
12/11/2024		1				1		
1/17/2025		1	1	1				
1/21/2025			1	1		1		
1/28/2025		1		1		1	1	
1/31/2025		1	1	1		2	1	1
2/5/2025			1			3		
2/11/2025			1			1	1	1
2/12/2025						1	1	1
2/13/2025			1	1		1		
2/18/2025		1		1	1	3	1	1
2/19/2025				1		1		
2/27/2025		1	1	1		3	2	
3/6/2025		1		1		1	1	1
3/13/2025		1				2	1	1
3/20/2025			1					
3/27/2025			1					
4/2/2025				1		1		
4/7/2025			1	1		1	1	
4/10/2025		1	1	1		1		
4/24/2025			1			1		
4/29/2025		1		1		1		

Date (d/m/y)	*Nostocoida limicola* III	T 0092	T 0803	T 021N	*Thiotrix* I	*Thiotrix* II	T 0914	*Beggiatoa spp.*
12/11/2024				1	1	1		1
1/17/2025		1		1	1			1
1/21/2025				1		1		1
1/28/2025				1	1			1
1/31/2025				1	2	1		1
2/5/2025		1		3	1			1
2/11/2025			1	1		1	1	
2/12/2025				1	1			
2/13/2025				1				1
2/18/2025				1	2	1		1
2/19/2025			1			1	1	
2/27/2025		1		1				1
3/6/2025			1	1		1		1
3/13/2025				1	1	1		1
3/20/2025						1		
3/27/2025			1				1	
4/2/2025						1		
4/7/2025		1		1				
4/10/2025		1		1		1		1
4/24/2025		1						
4/29/2025	1	1		3				

Date	*Mycothrix parvicella*	T 0581	*Nocardia spp.* e semelhantes

12/11/2024		1
1/17/2025	1	1
1/21/2025	1	1
1/28/2025	1	1
1/31/2025	1	2
2/5/2025	1	3
2/11/2025	3	2
2/12/2025	3	3
2/13/2025	2	2
2/18/2025	2	3
2/19/2025	1	1
2/27/2025	2	3
3/6/2025	2	3
3/13/2025	1	3
3/20/2025	1	1
3/27/2025	1	1
4/2/2025		1
4/7/2025	1	1
4/10/2025	1	1
4/24/2025	1	1
4/29/2025	1	3

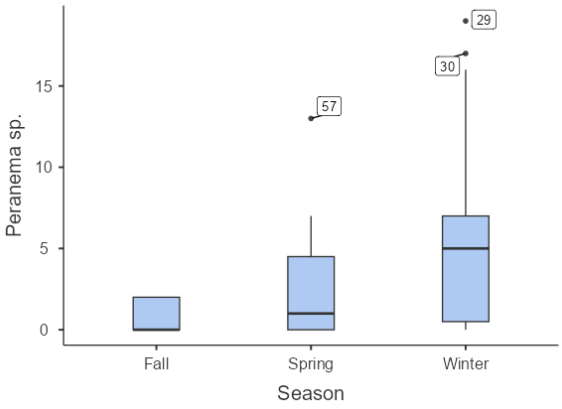
Peranema sp.
15
10
5
0
29
30
57
Fall
Spring
Winter
Season

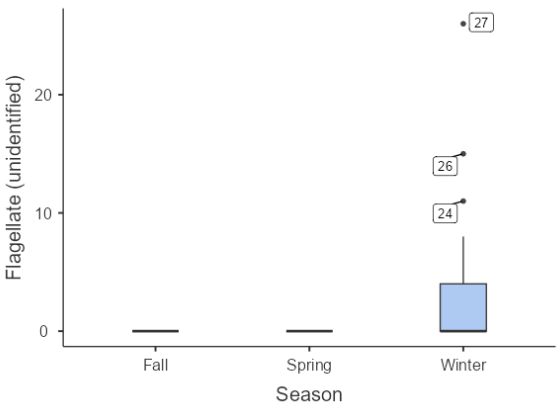
Flagellate (unidentified)
20
10
0
27
26
24
Fall
Spring
Winter
Season

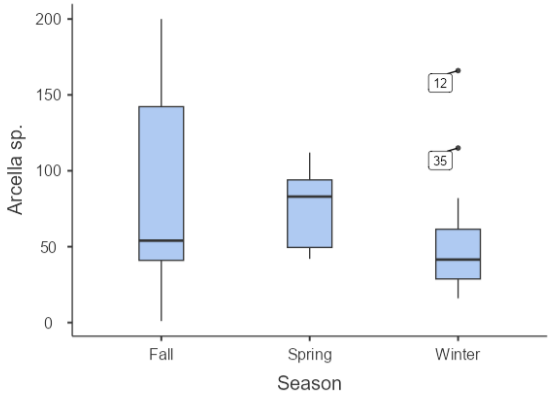
Arcella sp.
200
150
100
50
0
12
35
Fall
Spring
Winter
Season

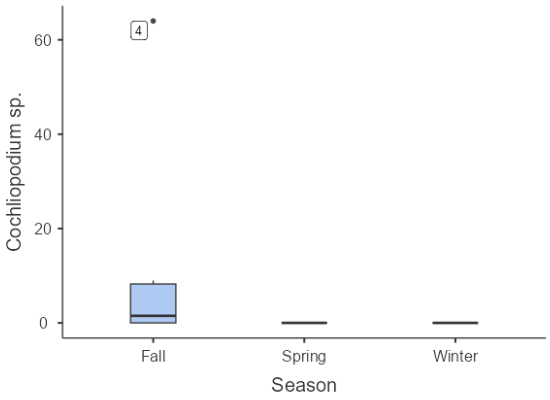
Cochliopodium sp.
60
40
20
0
4
Fall
Spring
Winter
Season

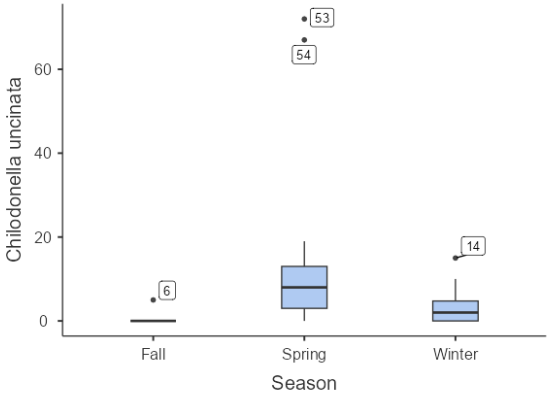
Chilodonella uncinata
60
40
20
0
53
54
14
6
Fall
Spring
Winter
Season

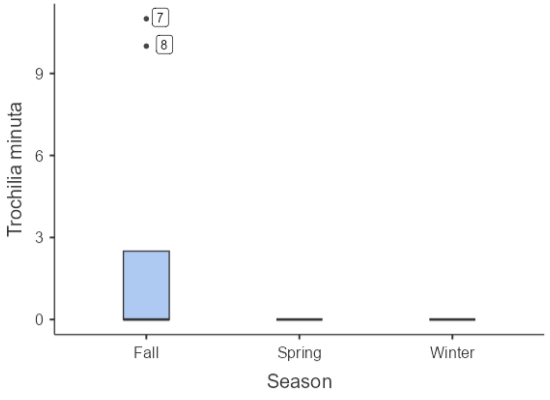
Trochilia minuta
9
6
3
0
7
8
Fall
Spring
Winter
Season

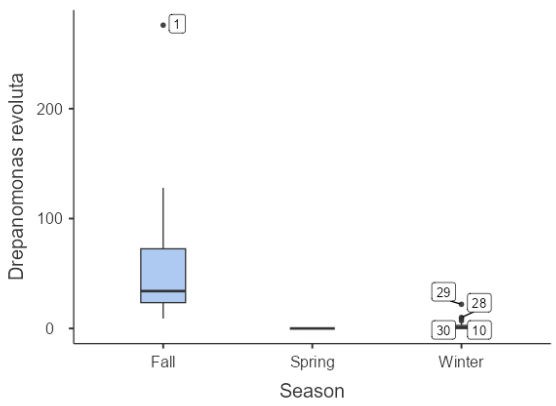
Drepanomonas revoluta
200
100
0
1
29
28
30
10
Fall
Spring
Winter
Season

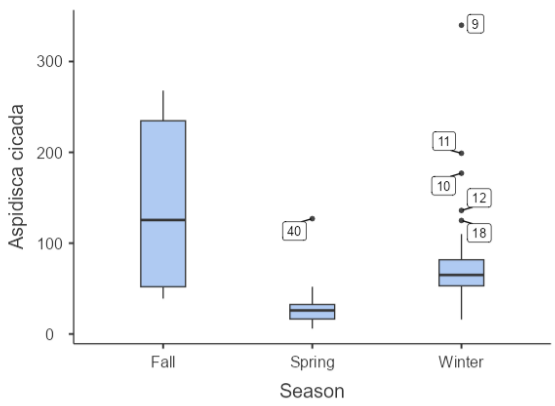
Aspidisca cicada
300
200
100
0
9
11
10
12
40
18
Fall
Spring
Winter
Season

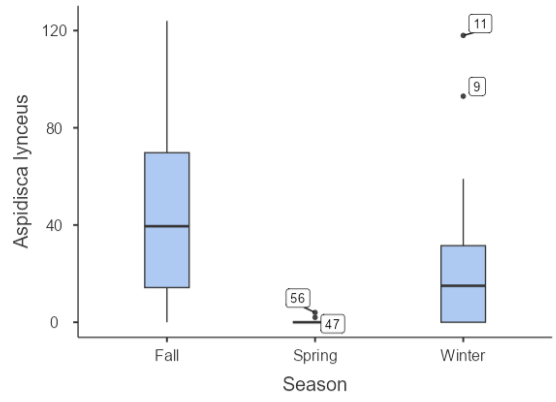
Aspidisca lynceus
120
80
40
0
11
9
56
47
Fall
Spring
Winter
Season

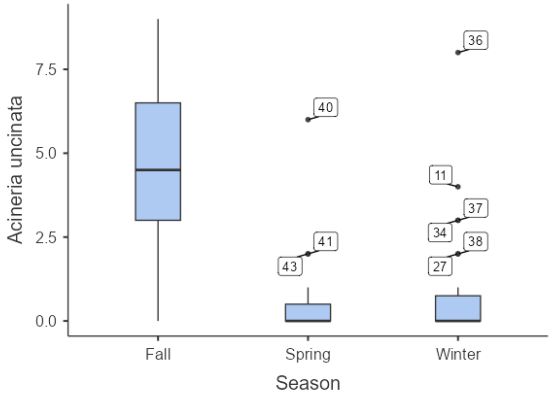
Acineria uncinata
7.5
5.0
2.5
0.0
36
40
11
37
34
41
38
43
27
Fall
Spring
Winter
Season

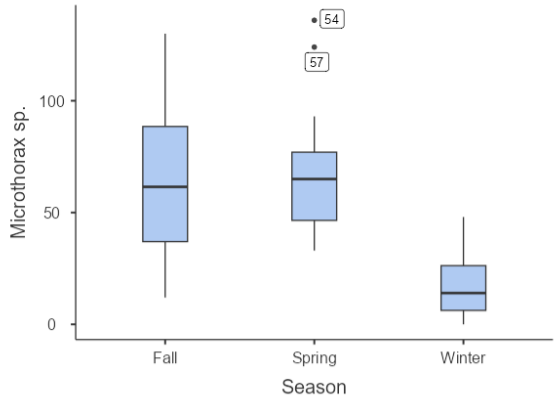
Microthorax sp.
100
50
0
54
57
Fall
Spring
Winter
Season

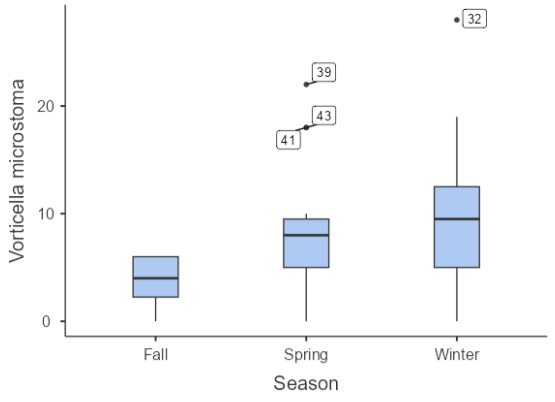
Vorticella microstoma
20
10
0
32
39
43
41
Fall
Spring
Winter
Season

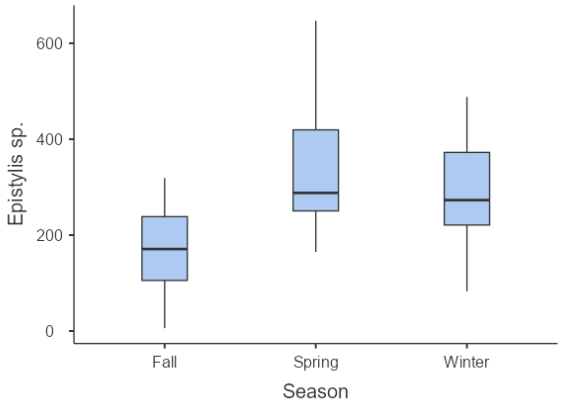
Epistylis sp.
600
400
200
0
Fall
Spring
Winter
Season

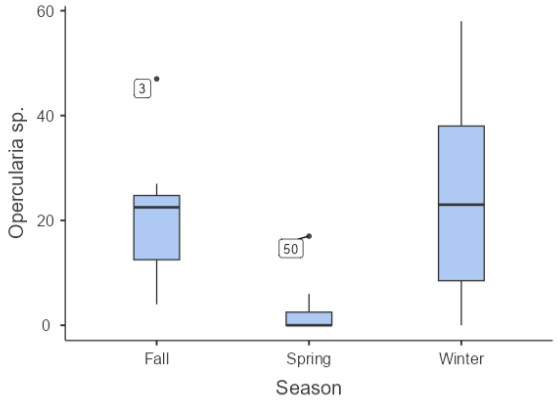
Opercularia sp.
60
40
20
0
3
50
Fall
Spring
Winter
Season

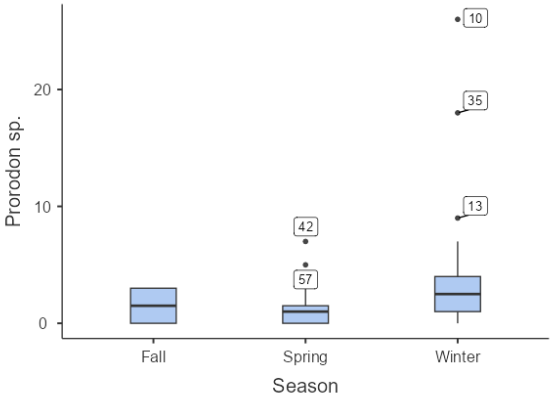
Prorodon sp.
20
10
0
10
35
13
42
57
Fall
Spring
Winter
Season

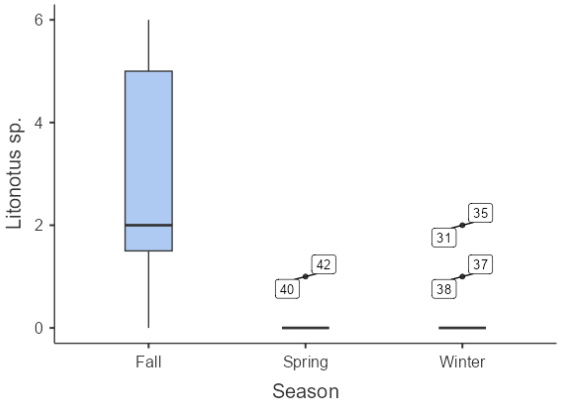
Litonotus sp.
6
4
2
0
35
31
42
40
37
38
Fall
Spring
Winter
Season

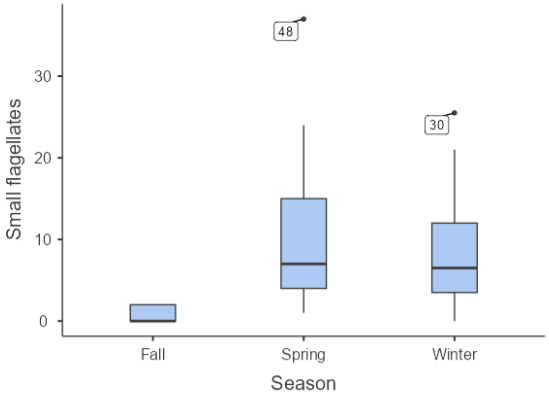
Small flagellates
30
20
10
0
48
30
Fall
Spring
Winter
Season

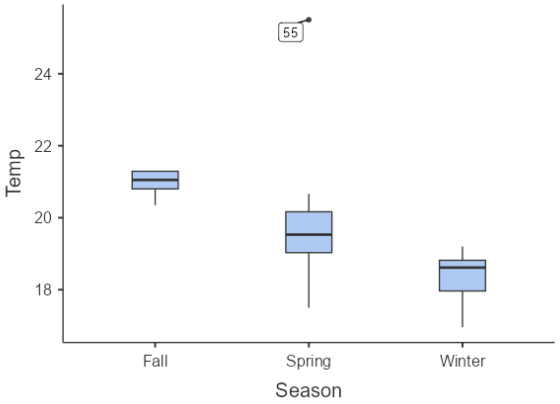
Temp
24
22
20
18
55
Fall
Spring
Winter
Season

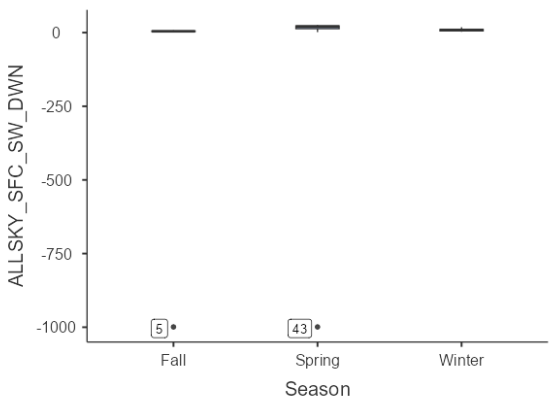
ALLSKY_SFC_SW_DWN
0
-250
-500
-750
-1000
5
43
Fall
Spring
Winter
Season

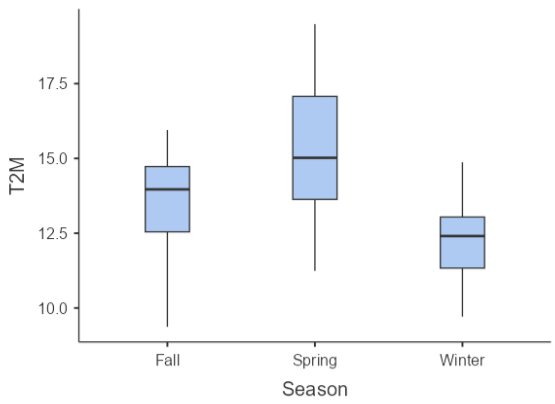
T2M
17.5
15.0
12.5
10.0
Fall
Spring
Winter
Season

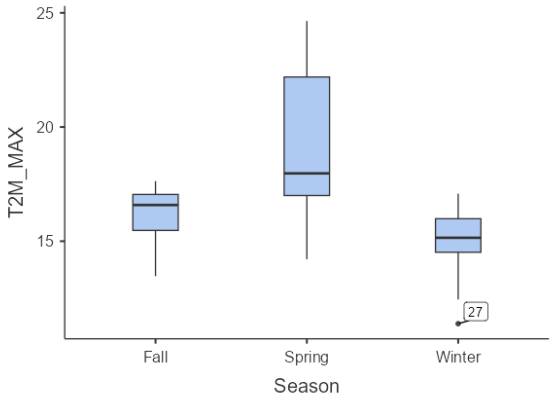
T2M_MAX
25
20
15
27
Fall
Spring
Winter
Season

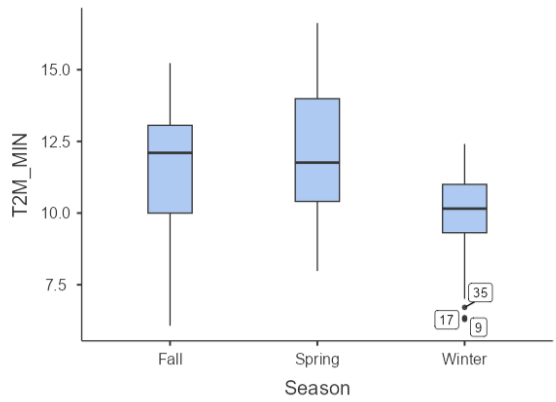
T2M_MIN
15.0
12.5
10.0
7.5
35
17
9
Fall
Spring
Winter
Season

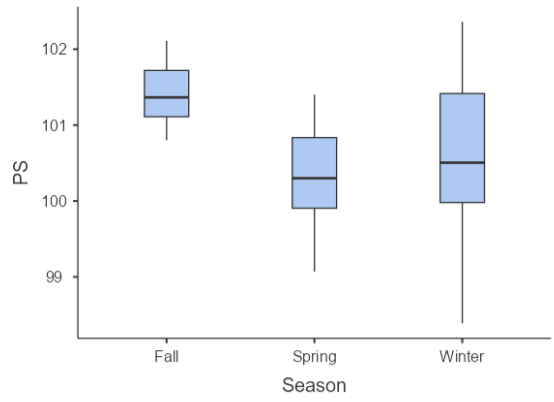
PS
102
101
100
99
Fall
Spring
Winter
Season

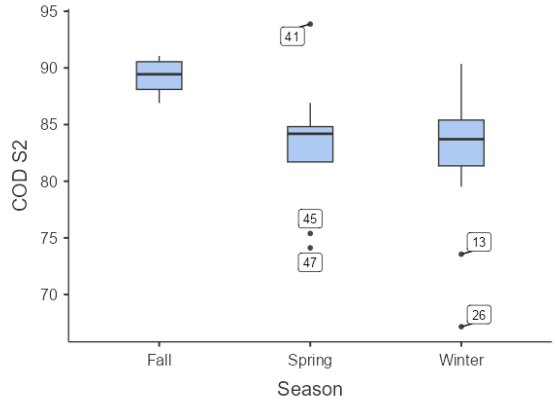
COD S2
95
90
85
80
75
70
41
45
47
13
26
Fall
Spring
Winter
Season

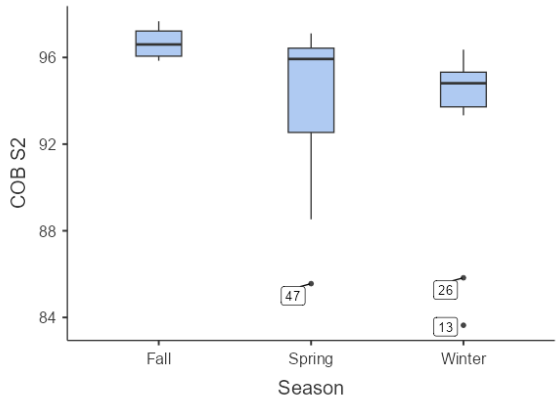
COB S2
96
92
88
84
47
26
13
Fall
Spring
Winter
Season

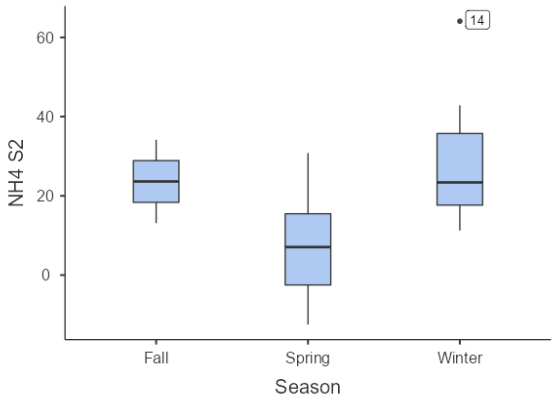
NH4 S2
60
40
20
0
14
Fall
Spring
Winter
Season

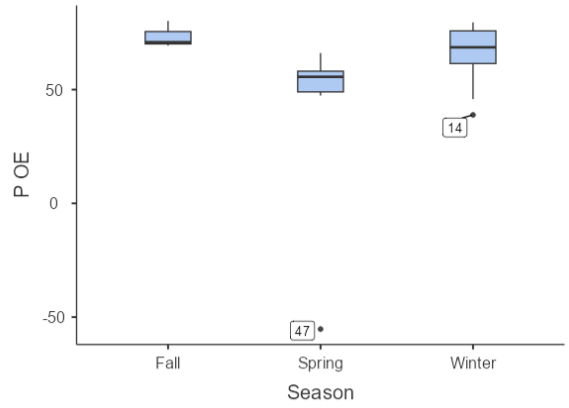
P OE
50
0
-50
14
47
Fall
Spring
Winter
Season

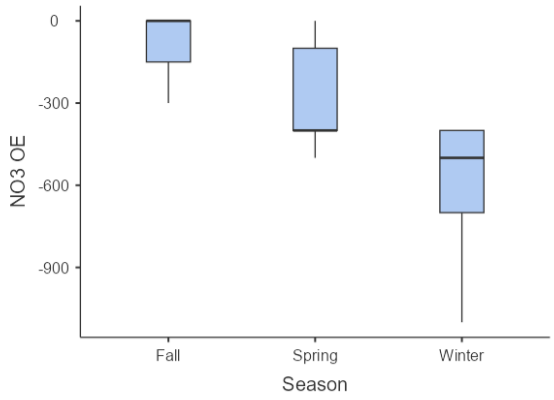
NO3 OE
0
-300
-600
-900
Fall
Spring
Winter
Season

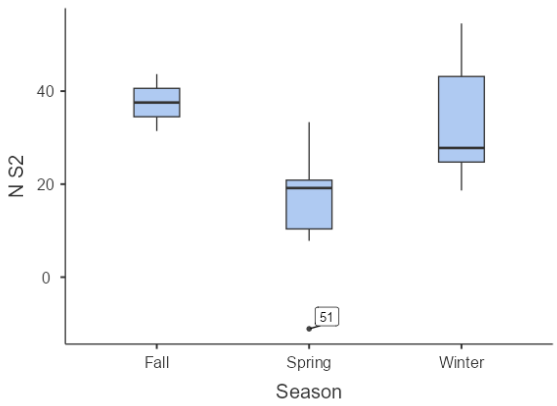
N S2
40
20
0
51
Fall
Spring
Winter
Season

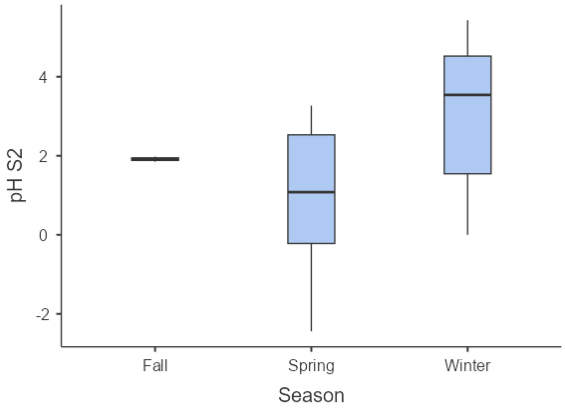
pH S2
4
2
0
-2
Fall
Spring
Winter
Season

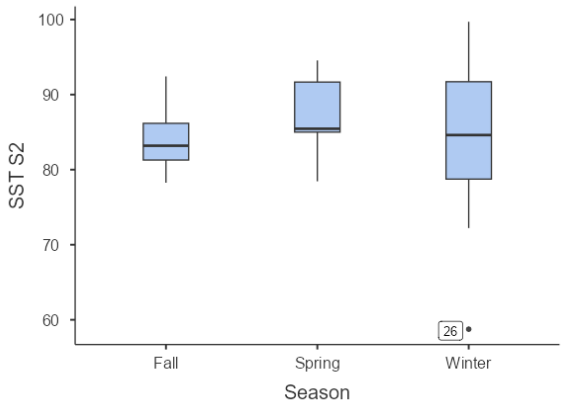

Annex 3 Seasonal Comparison Boxplots of Variables With Significant Pairwise Differences. This annex displays boxplots for all variables showing at least one statistically significant seasonal difference based on pairwise comparisons, as well as for all removal efficiency variables. Made with Jamovi.

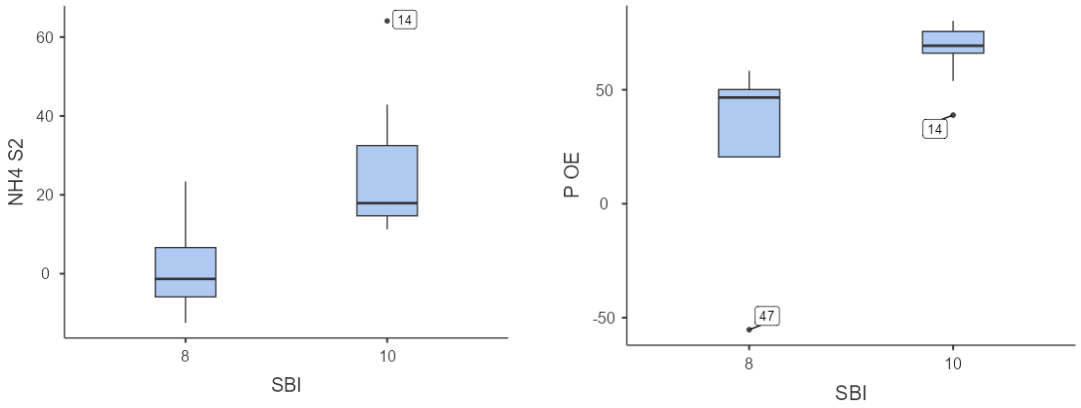

Annex 4 Boxplots of Sludge Biotic Index (SBI) in Relation to NH_4^+ S2 and Total P OE Variables. Boxplots comparing SBI scores with ammonium (NH_4^+) at Sedipac 3D #2 (S2) and total phosphorus (P) at the Affluent (OE). Made in Jamovi.

Note. OE = Affluent. S2 = Sedipac 3D #2. NH_4^+ = Ammonium.

Annex 5 R Script for Dunn's Test. This annex includes the R script used for the post hoc Dunn test, used in RStudio. Based on: https://www.youtube.com/watch?v=pyLQmUfrel8.

```
# Load libraries
library(FSA)
library(dunn.test)

# Vector of variables to compare with Season or SBI
vars <- c("variables")

# Apply Kruskal-Wallis and then Dunn only if p < 0.05
for (v in vars) {
  f <- as.formula(paste(v, "~ Season/SBI"))
  kr <- kruskal.test(f, data = myData)

  if (kr$p.value < 0.05) {
    cat("\n==== Dunn Test (Holm) for:", v, "====\n")
    print(dunnTest(f, data = myData, method = "holm"))
  }
}
```

Annex 6 Correlation Matrix With p-Values Between Environmental and Process Variables. This annex presents the p-value matrix for pairwise correlations. Green cells indicate statistically significant correlations ($p < .05$). Made with Jamovi.

	Peranema spp.	Flagellate (unidentified)	*Arcella spp.*	*Cochliopodium spp.*	*Trochilia minuta*	*Drepanomonas revoluta*	*Aspidisca cicadas*	*Aspidisca lynceus*	*Acineria uncinata*	*Microthorax spp.*	*Vorticella microstoma*
O_2	0.98	0.378	0.23	0.15	0.386	0.041	0.452	0.12	0.404	0.546	0.085
Temp (C°)	0.688	0.222	0.45	0.028	0.054	0.969	<.001	0.096	0.378	<.001	0.035
ALLSKY_SFC_SW_DWN %	0.791	0.417	0.192	0.021	0.577	0.002	<.001	0.003	0.027	0.044	0.968
T2M (C°)	0.049	0.014	<.001	0.064	0.02	0.079	0.005	0.01	0.512	<.001	0.153
T2M_MAX (C°)	0.026	0.005	<.001	0.203	0.04	0.176	0.001	0.006	0.599	<.001	0.26
T2M_MIN (C°)	0.074	0.044	0.017	0.048	0.029	0.326	0.097	0.172	0.477	0.008	0.08
PRECTOTCORR (mm/day)	0.038	0.379	0.279	0.796	0.082	0.907	0.188	0.835	0.724	0.312	0.144
RH2M	0.722	0.32	0.36	0.169	0.655	0.281	0.001	0.487	0.344	0.411	0.994
PS (hPa)	0.013	0.126	0.008	0.051	0.317	0.008	0.017	0.009	0.892	0.114	0.418
COD S2 (mg/L)	0.343	0.345	0.528	0.013	NaN	0.184	0.109	0.113	0.019	0.254	0.347
COB S2 (mg/L)	0.329	0.357	0.033	0.051	NaN	0.566	0.574	0.72	0.043	0.016	0.813
NH_4^+ S2 (mg/L)	0.254	0.068	0.408	0.629	NaN	0.125	0.351	0.227	1	0.17	0.371
NO_3^- OE (mg/L)	0.694	0.096	0.286	0.022	NaN	0.2	0.724	0.63	0.007	0.002	0.07
P OE (mg/L)	0.209	0.564	0.943	0.09	NaN	0.283	<.001	0.084	0.322	0.448	0.581
N S2 (mg/L)	0.732	0.299	0.466	0.236	NaN	0.027	0.084	0.045	0.423	0.155	0.78
pH S2 (mg/L)	0.569	0.607	0.259	0.993	NaN	0.369	0.226	0.086	0.177	0.103	0.608
TSS S2 (mg/L)	0.883	0.461	0.625	0.874	NaN	0.23	0.358	0.587	0.98	0.353	0.419

	Carchesium spp.	*Epistylis spp.*	*Opercularia spp.*	*Prorodon spp.*	*Litonotus spp.*	*Podophrya spp.*	*Tokophrya spp.*	Rotifer (Digononta) *Rotaria spp.*	Rotifer (Monogononta) *spp.*	*Proales* Nematode
O3	0.885	0.643	0.25	0.072	0.294	0.157	0.194	0.449	0.575	0.626
Temp (C°)	0.205	0.329	0.103	0.037	0.206	0.731	0.561	0.176	0.458	0.111
ALLSKY_SFC_SW_DWN %	0.562	0.072	0.002	0.135	0.069	0.195	0.016	0.768	0.355	0.058
T2M (C°)	0.049	0.812	0.044	0.007	0.971	0.097	0.859	0.061	0.175	0.797
T2M_MAX(C°)	0.183	0.524	0.016	0.011	0.711	0.431	0.53	0.409	0.055	0.866
T2M_MIN(C°)	0.02	0.903	0.265	0.101	0.837	0.059	0.555	0.072	0.386	0.277
PRECTOTCORR (mm/day)	0.801	0.98	0.351	0.656	0.77	0.195	0.811	0.31	0.947	0.201
RH2M	0.637	0.576	0.02	0.634	0.59	0.923	0.173	0.749	0.912	0.652
PS (hPa)	0.68	0.016	0.003	0.935	0.292	0.023	0.772	0.005	0.164	0.75
COD S2	0.518	0.864	0.165	0.892	0.038	0.615	0.324	0.679	0.237	0.929
COB S2	0.533	0.177	0.865	0.804	0.199	0.417	0.584	0.971	0.923	0.877
NH_4^+ S2	NaN	0.732	0.05	0.627	0.476	0.921	0.644	0.927	0.02	0.826
NO_3^- OE	0.179	0.802	0.182	0.675	0.033	0.711	0.744	0.568	0.108	0.911
P OE	0.432	0.383	<.001	0.073	0.358	0.244	0.032	0.741	1	0.309
N S2	NaN	0.314	0.003	0.051	0.296	0.514	0.657	0.969	0.021	0.374
pH S2	NaN	0.961	0.01	0.223	0.598	0.912	0.73	0.911	0.02	0.467
TSS S2	0.565	0.194	0.899	0.76	0.82	0.07	0.765	0.688	0.055	0.018

	Small Flagellates	**Microfauna Density**
O_2	0.402	0.734

Temp (C°)	0.499	0.306
ALLSKY_SFC_SW_DWN %	0.049	0.491
T2M (C°)	0.612	0.217
T2M_MAX(C°)	0.31	0.378
T2M_MIN(C°)	0.975	0.215
PRECTOTCORR (mm/day)	0.818	0.472
RH2M	0.323	0.067
PS (hPa)	0.004	0.464
COD S2 (mg/L)	0.033	0.027
COB S2 (mg/L)	0.037	<.001
NH_4^+ S2 (mg/L)	0.034	0.718
NO_3^- OE (mg/L)	0.864	0.14
P OE (mg/L)	0.008	0.322
N S2 (mg/L)	0.034	0.793
pH S2 (mg/L)	0.341	0.587
TSS S2 (mg/L)	0.884	0.564

Note. Abbreviations:

- S2 = Sedipac 3D #2
- OE = Affluent
- O_2 = Dissolved oxygen (Oxymax COS61D sensor)
- Temp = Temperature (Oxymax COS61D sensor)
- TSS = Total Suspended Solids
- COD = Chemical Oxygen Demand
- COB = Biochemical Oxygen Demand
- NH_4^+ = Ammonium
- NO_3^- = Nitrate
- Total P = Total Phosphorus
- Total N = Total nitrogen
- ALLSKY_SFC_SW_DWN = Downward shortwave solar radiation under all-sky conditions
- T2M, T2M max, T2M min = Air temperature (mean, max, min) at 2 meters
- PRECTOTCORR = Corrected total precipitation
- RH2M = Relative humidity at 2 meters

PS = Surface atmospheric pressure

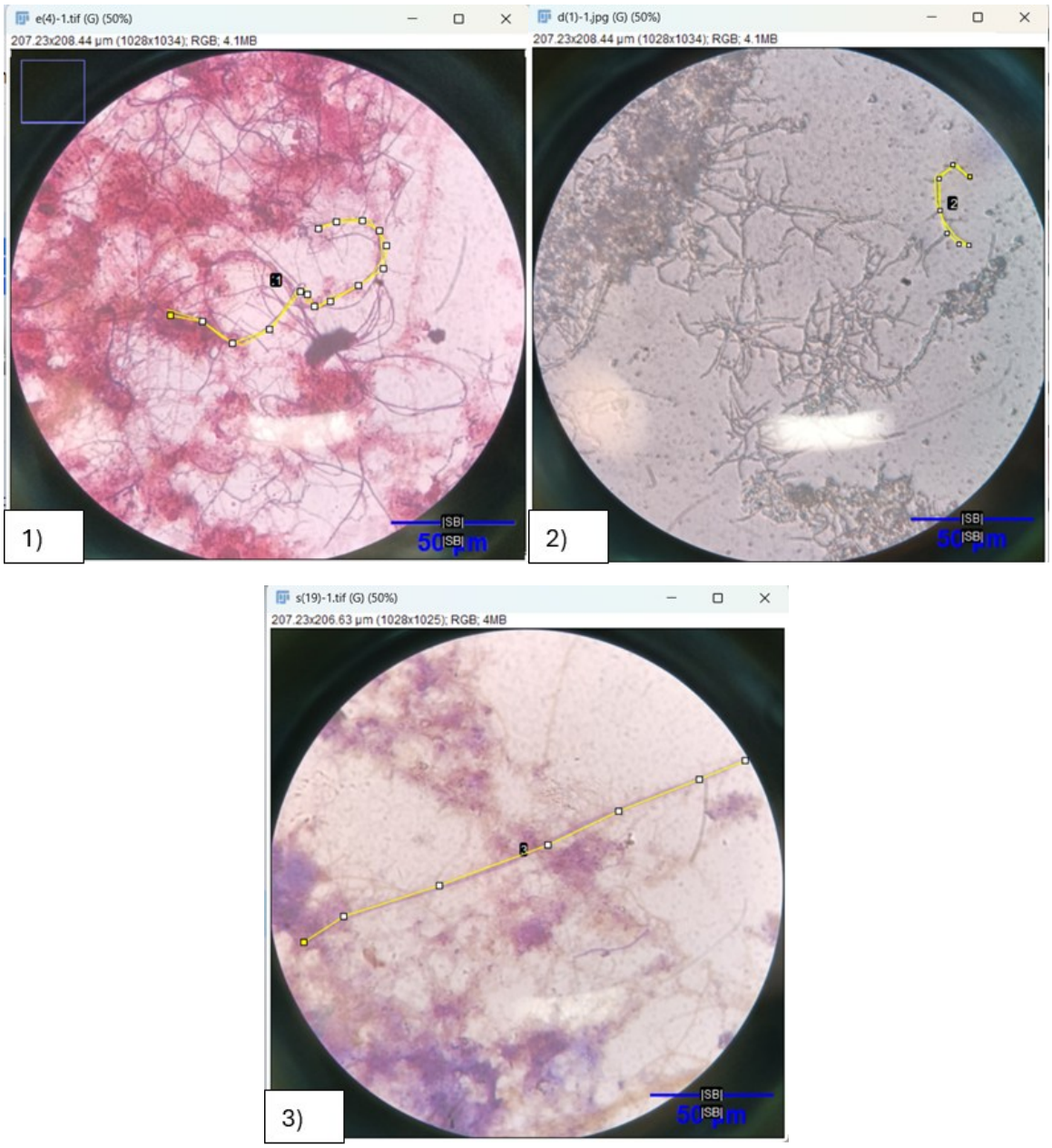

Annex 7 Microscopic Images of Selected Filamentous Bacteria

1. *Microthrix parvicella*, Gram-stained (Gram-positive), observed on 31/01/2025.
2. *Nocardia* spp. and morphologically similar organisms under direct observation, observed on 28/01/2025.
3. Type 0041, stained with Neisser stain (positive only in the filament), observed on 10/04/2025.

Note. All images were analyzed using ImageJ software.

Annex 8 Morphometric Measurements of Filamentous Bacteria Images (From Annex 7) This annex provides length, width, and other morphometric data obtained from the microscopic images using ImageJ.

Photo	Label	Length (µm)
1	*Microthrix parvicella*	146.722
2	*Nocardia spp.*	49.588
3	T0041	193.776

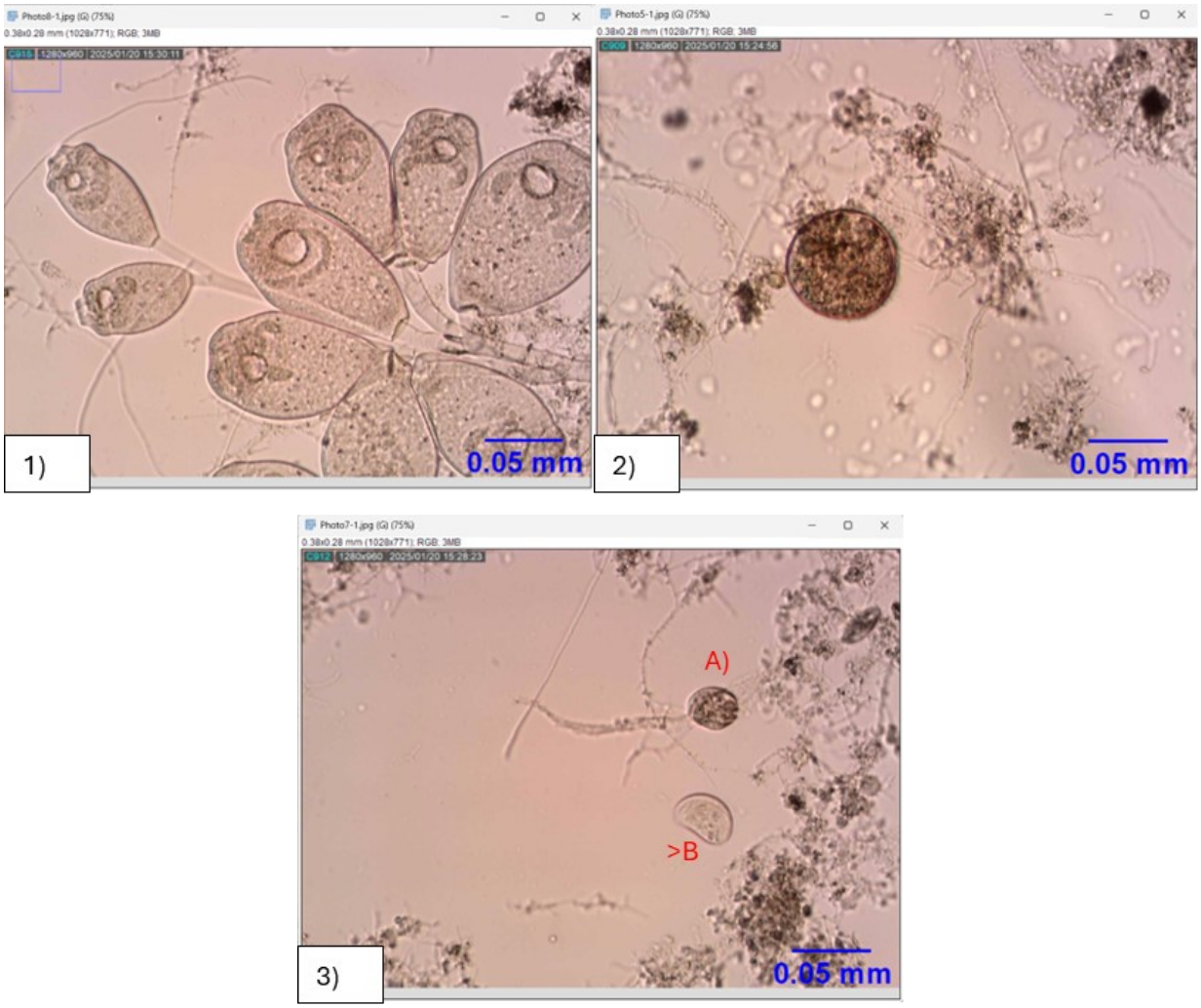

Annex 9 Microscopic Images of Protozoa and Metazoan Taxa. Includes images of:

1. *Epistylis* spp.
2. *Arcella* spp.
3. a) *Aspidisca cicada*, b) *Microthorax* spp.

Captured with a DinoEye C-Mount Microscope Camera. Scale bars added with ImageJ.

Observation date: 20/01/2025.

Annex 10 Descriptive Statistics of Environmental, Biological, and Process Variables. This annex presents the descriptive statistics for the variables analyzed in the study, including environmental parameters, biological reactor conditions, protozoa presence, removal efficiencies, and differences between Affluent and intermediate treatment points. Unless otherwise stated, the total number of observations for each variable is $N = 57$. Standard deviations (SD) are provided where applicable. Made with Jamovi.

Environmental Variables. These variables describe ambient conditions relevant to wastewater treatment performance.

- **ALLSKY_SFC_SW_DWN**: Downward shortwave solar radiation under all-sky conditions (W/m^2).
- **T2M**: Mean air temperature at 2 meters (°C).
- **T2M max**: Maximum air temperature at 2 meters (°C).
- **T2M min**: Minimum air temperature at 2 meters (°C).
- **PRECTOTCORR**: Corrected total precipitation (mm).
- **RH2M**: Relative humidity at 2 meters (%).
- **PS**: Atmospheric pressure at the Earth's surface (Pa).

	ALLSKY_SFC_SW_DWN %	T2M (C°)	T2M_MAX (C°)	T2M_MIN (C°)	PRECTOTCORR (mm/day)	RH2M %	PS (hPa)
Mean	-24.1	13.4	16.5	10.8	3.02	83.2	101
SD	188	2.35	2.85	2.41	5.35	6.79	0.902
Median	9.45	13.1	16.1	10.8	0.68	85	101
Min	-999	9.37	11.4	6.07	0	67.6	98.4
Max	25.9	19.5	24.6	16.6	26.4	95.3	102
Shapiro-Wilk W	0.209	0.952	0.886	0.983	0.605	0.955	0.986
Shapiro-Wilk p-value	<.001	0.024	<.001	0.579	<.001	0.032	0.734

Biological Reactor Variables (BRs). Measurements related to the internal operational conditions of the biological reactors.

- **O_2**: Dissolved oxygen (mg/L), measured using an Oxymax COS61D sensor.

- **Temp**: Temperature (°C), also measured with the Oxymax COS61D sensor.

	O_2	**Temp**
N	53	54
Mean	0.914	19.1
SD	0.455	1.4
Median	0.81	18.8
Min	0.02	17
Max	1.74	25.5
Shapiro-Wilk W	0.964	0.866
Shapiro-Wilk p-value	0.111	<.001

Protozoa Variables. Descriptive data related to protozoan abundance and/or presence, derived from microscopy-based observations.

	***Peranema* spp.**	**Flagellate (unidentified)**	***Arcella* spp.**	***Cochliopodium* spp.**	***Tetrahymena pyriformis***	***Sathrophilus* spp.**	***Chilodonella uncinata***	***Trochilia minuta***	***Drepanomonas revoluta***	***Aspidisca cicada***
Mean	3.75	1.63	63.7	1.47	0.211	1.04	6.42	0.368	11.5	73.5
SD	4.71	4.4	39.5	8.58	1.59	7.81	13	1.95	40.6	70.1
Median	2	0	54	0	0	0	3	0	0	53
Min	0	0	1	0	0	0	0	0	0	6
Max	19	26	200	64	12	59	72	11	276	340
Shapiro-Wilk W	0.781	0.435	0.898	0.166	0.114	0.114	0.468	0.183	0.304	0.761
Shapiro-Wilk p-value	<.001	<.001	<.001	<.001	<.001	<.001	<.001	<.001	<.001	<.001
25th percentile	0	0	39	0	0	0	0	0	0	29

50th percentile	2	0	54	0	0	0	3	0	0	53
75th percentile	5	0	83	0	0	0	7	0	3	75

	Aspidisca lynceus	*Euplotes patella*	*Euplotes affinis*	*Acineria uncinata*	*Microthorax spp.*	*Vorticella microstoma*	*Vorticella infusionum*	*Vorticella aquadulcis*	*Vorticella convallaria*	*Carchesium spp.*
Mean	18.1	0.0175	0.0351	1.3	40.5	8.19	0.158	3.3	2.56	0.719
SD	29.8	0.132	0.265	2.31	34	5.84	1.19	2.77	2.53	2.58
Median	0	0	0	0	34	8	0	3	2	0
Min	0	0	0	0	0	0	0	0	0	0
Max	124	1	2	9	136	28	9	14	11	17
Shapiro-Wilk W	0.672	0.114	0.114	0.635	0.901	0.929	0.114	0.899	0.865	0.314
Shapiro-Wilk p-value	<.001	<.001	<.001	<.001	<.001	0.003	<.001	<.001	<.001	<.001
25th percentile	0	0	0	0	12	5	0	1	0	0
50th percentile	0	0	0	0	34	8	0	3	2	0
75th percentile	26	0	0	2	63	11	0	5	5	0

	Zoothamnium spp.	*Epistylis spp.*	*Opercularia spp.*	*Prorodon spp.*	*Colpeps hirtus*	*Litonotus spp.*	*Podophrya spp.*	*Tokophrya spp.*	**Rotifer (Digononta)**	**Rotifer (Monogononta)**

									Rotaria spp.	*Lepadella spp.*
Mean	1.21	295	15.8	2.7	0.0351	0.526	0.386	0.509	1.91	0.0351
SD	4.07	137	17.1	4.35	0.265	1.3	0.796	0.869	2.27	0.265
Median	0	270	10	2	0	0	0	0	1	0
Min	0	6	0	0	0	0	0	0	0	0
Max	23	647	58	26	2	6	4	3	10	2
Shapiro-Wilk W	0.334	0.947	0.849	0.592	0.114	0.469	0.548	0.63	0.808	0.114
Shapiro-Wilk p-value	<.001	0.014	<.001	<.001	<.001	<.001	<.001	<.001	<.001	<.001
25th percentile	0	220	1	0	0	0	0	0	0	0
50th percentile	0	270	10	2	0	0	0	0	1	0
75th percentile	0	353	26	3	0	0	1	1	3	0

	Rotifer (Monogononta) *Proales spp.*	**Rotifer (Monogononta) *Cephalodella spp.***	**Nematode**	**Oligochaeti**	**Tardigrade**	**Small Flagellates**	**Microfauna Density**
Mean	0.281	0.0175	0.474	0.0877	0.0175	7.98	1.12E+07
SD	1.06	0.132	1.14	0.342	0.132	7.91	3.50E+06
Median	0	0	0	0	0	5.5	10500000
Min	0	0	0	0	0	0	5400000
Max	6	1	5	2	1	37	20000000

Shapiro-Wilk W	0.292	0.114	0.484	0.27 9	0.114	0.86	0.942
Shapiro-Wilk p-value	<.001	<.001	<.001	<.00 1	<.001	<.001	0.009
25th percentile	0	0	0	0	0	2	8.90E+06
50th percentile	0	0	0	0	0	5.5	1.05E+07
75th percentile	0	0	0	0	0	12	1.28E+07

Removal Efficiency Variables (mg/L). These values represent the concentrations of key water quality parameters before (OE = Affluent) and after partial treatment (S2 = Sedipac 3D #2).

- **TSS**: Total Suspended Solids
- **COD**: Chemical Oxygen Demand
- **COB**: Biochemical Oxygen Demand
- **NH_4^+**: Ammonium
- **NO_3^-**: Nitrate
- **Total P**: Total Phosphorus
- **Total N**: Total Nitrogen

	COD OE	**COD S2**	**COB OE**	**COB S2**	**NH_4^+ OE**	**NH_4^+ S2**	**NO_3^- OE**	**P OE**	**N OE**	**N S2**	**pH OE**	**pH S2**	**TSS OE**	**TSS S2**
N	57	25	27	25	16	15	17	17	17	15	30	16	57	25
Mean	87.8	83.6	95.8	94	21.7	19.9	-394	57	32.1	26.8	1.33	2.1	89.3	84.9
SD	3.8	6.05	2.3	3.88	13	19	290	31.3	12.5	16.2	1.73	2.1	7.56	8.42
Median	88	84.3	96.5	95.4	22.9	17.4	-400	66.7	30.4	27.3	1.15	1.92	91.7	85
Min	77.4	67.2	87.8	83.6	5.12	-12.5	-1100	-55.3	7.41	-11.1	-1.85	-2.44	65.5	58.8
Max	94.7	93.9	98.6	97.7	44	64.1	0	80.2	50	54.5	4.26	5.43	99.6	99.7
Shapiro-Wilk W	0.98	0.93	0.83	0.74	0.92	0.97	0.89	0.62	0.94	0.96	0.97	0.98	0.85	0.92
Shapiro-Wilk p-value	0.51	0.09	<.001	<.001	0.18	0.82	0.04	<.001	0.39	0.67	0.46	0.97	<.001	0.05

Differences Between S2 and OE (mg/L). This section provides descriptive statistics of the concentration differences between Affluent (OE) and intermediate treatment point (S2) for the following variables:

- **TSS**
- **COB**
- **NH_4^+**

	COD	**COB**	**NH_4^+**	**N**	**pH**	**TSS**
Asymmetry	1.16	1.91	-0.62	0.132	-0.29	-0.37
Estimated error asymmetry	0.464	0.46	0.580	0.580	0.56	0.46
Shapiro-Wilk W	0.913	0.75	0.968	0.975	0.94	0.97
Shapiro-Wilk p-value	0.036	<.001	0.826	0.923	0.30	0.71

Note. Positive values indicate a higher concentration in the Affluent (OE) compared to Sedipac 3D #2 (S2), reflecting effective removal.

Annex 11 Seasonal Comparison of Variables With Significant Dunn Test Results (Holm-Adjusted p-values). This annex includes only variables that showed at least one significant pairwise seasonal difference. Dunn test was used with Holm correction. Made with Jamovi.

Note.

- OE = Affluent
- S2 = Sedipac 3D #2
- Temp = Temperature (Oxymax COS61D sensor)
- NO_3^- = Nitrate
- ALLSKY_SFC_SW_DWN = Downward shortwave radiation
- T2M, T2M max, T2M min = Air temperature
- PS = Surface atmospheric pressure

Genus / Variable	Comparison	Z	P unadjusted	P tight Holm
	Fall - Spring	-1.076	0.2818	0.2818
	Fall - Winter	-2.749	0.006	0.0179
	Spring -			
Peranema spp.	Winter	-2.184	0.029	0.058
	Fall - Spring	0	1	1
	Fall - Winter	-2.666	0.0077	0.0153
	Spring -			
Flagellate (unidentified)	Winter	-3.618	0.0003	0.0009
	Fall - Spring	-0.808	0.4191	0.4191
	Fall - Winter	1.513	0.1303	0.2605
	Spring -			
Arcella spp.	Winter	3.215	0.0013	0.0039
	Fall - Spring	4.6	4.23E-06	8.47E-06
	Fall - Winter	4.872	1.11E-06	3.32E-06
	Spring -			
Cochliopodium spp.	Winter	0	1	1
	Fall - Spring	-3.98	6.89E-05	0.0002
Chilodonella uncinata	Fall - Winter	-2.05	0.0403	0.0403

	Spring - Winter	2.938	0.0033	0.0066
	Fall - Spring	3.195	0.0014	0.0028
	Fall - Winter	3.384	0.0007	0.0021
Trochilia minuta	Spring - Winter	0	1	1
	Fall - Spring	5.734	9.79E-09	2.94E-08
	Fall - Winter	3.962	7.44E-05	0.0001
Drepanomonas revoluta	Spring - Winter	-2.866	0.0042	0.0042
	Fall - Spring	4.01	6.08E-05	0.0001
	Fall - Winter	0.979	0.3273	0.3273
Aspidisca cicada	Spring - Winter	-4.435	9.23E-06	2.77E-05
	Fall - Spring	4.067	4.76E-05	0.0001
	Fall - Winter	1.671	0.0947	0.0947
Aspidisca lynceus	Spring - Winter	-3.579	0.0003	0.0007
	Fall - Spring	3.736	0.0002	0.0004
	Fall - Winter	3.848	0.0001	0.0004
Acineria uncinata	Spring - Winter	-0.148	0.8822	0.8822
	Fall - Spring	-0.46	0.6455	0.6455
	Fall - Winter	3.51	0.0004	0.0009
Microthorax spp.	Spring - Winter	5.425	5.78E-08	1.74E-07
	Fall - Spring	-2.023	0.043	0.0861
Vorticella microstoma	Fall - Winter	-2.882	0.004	0.0119

	Spring - Winter	-1.002	0.3162	0.3162
	Fall - Spring	-2.826	0.0047	0.0141
	Fall - Winter	-2.384	0.0171	0.0343
Epistylis spp.	Spring - Winter	0.828	0.4078	0.4078
	Fall - Spring	3.294	0.001	0.002
	Fall - Winter	0.07	0.9443	0.9443
Opercularia spp.	Spring - Winter	-4.641	3.47E-06	1.04E-05
	Fall - Spring	0.491	0.6234	0.6234
	Fall - Winter	-1.364	0.1725	0.345
Prorodon spp.	Spring - Winter	-2.557	0.0106	0.0317
	Fall - Spring	4.15	3.33E-05	6.66E-05
	Fall - Winter	4.185	2.85E-05	8.54E-05
Litonotus spp.	Spring - Winter	-0.285	0.7756	0.7756
	Fall - Spring	-3.73	0.0002	0.0006
	Fall - Winter	-3.555	0.0004	0.0008
Small Flagellates	Spring - Winter	0.538	0.5908	0.5908
	Fall - Spring	1.878	0.0604	0.0604
	Fall - Winter	4.187	2.82E-05	8.46E-05
Temp (C°)	Spring - Winter	3.68	0.0002	0.0005
	Fall - Spring	-4.2739	1.92E-05	5.76E-05
ALLSKY_SFC_SW_DWN %	Fall - Winter	-2.0775	3.78E-02	3.78E-02

	Spring - Winter	3.3242	8.87E-04	1.77E-03
	Fall - Spring	-1.4681	1.42E-01	1.42E-01
	Fall - Winter	1.8838	5.96E-02	1.19E-01
T2M (C°)	Spring - Winter	4.667	3.06E-06	9.17E-06
	Fall - Spring	-1.9167	5.53E-02	1.11E-01
	Fall - Winter	1.6454	9.99E-02	9.99E-02
T2M_MAX (C°)	Spring - Winter	4.9882	6.09E-07	1.83E-06
	Fall - Spring	-0.4416	6.59E-01	6.59E-01
	Fall - Winter	1.8606	6.28E-02	1.26E-01
T2M_MIN (C°)	Spring - Winter	3.1598	1.58E-03	4.74E-03
	Fall - Spring	2.9626	3.05E-03	9.15E-03
	Fall - Winter	2.2561	2.41E-02	4.81E-02
PS (hPa)	Spring - Winter	-1.1967	2.31E-01	2.31E-01
	Fall - Spring	2.2485	2.45E-02	4.91E-02
	Fall - Winter	2.4122	1.59E-02	4.76E-02
COD.S2	Spring - Winter	0.0942	9.25E-01	9.25E-01
	Fall - Spring	1.1321	2.58E-01	2.58E-01
	Fall - Winter	2.7486	5.99E-03	1.80E-02
NO_3^-.OE	Spring - Winter	1.9632	4.96E-02	9.92E-02